

Theory of wave-packet transport under narrow gaps and spatial textures: Nonadiabaticity and semiclassicality

Matisse Wei-Yuan Tu ^{*}, Ci Li, and Wang Yao

*Department of Physics, The University of Hong Kong, Hong Kong, China
and HKU-UCAS Joint Institute of Theoretical and Computational Physics at Hong Kong, China*



(Received 8 April 2020; accepted 18 June 2020; published 22 July 2020)

We generalize the celebrated semiclassical wave-packet approach from the adiabatic to the nonadiabatic regime. A unified description covering both of these regimes is particularly desired for systems with spatially varying band structures where band gaps of various sizes are simultaneously present, e.g., in moiré patterns. For a single wave packet, alternative to the previous derivation by Lagrangian variational approach, we show that the same semiclassical equations of motion can be obtained by introducing a spatial-texture-induced force operator similar to the Ehrenfest theorem. For semiclassically computing the current, the ensemble of wave packets based on adiabatic dynamics is shown to well correspond to a phase-space fluid for which the fluid's mass and velocity are two distinguishable properties. This distinction is not inherited to the ensemble of wave packets with the nonadiabatic dynamics. We extend the adiabatic kinetic theory to the nonadiabatic regime by taking into account decoherence, whose joint action with electric field favors certain forms of interband coherence. The steady-state density matrix as a function of the phase-space variables is then phenomenologically obtained for calculating the current. The result, applicable with a finite electric field, expectedly reproduces the known adiabatic limit by taking the electric field to be infinitesimal, and therefore attains a unified description from the adiabatic to the nonadiabatic situations.

DOI: [10.1103/PhysRevB.102.045423](https://doi.org/10.1103/PhysRevB.102.045423)

I. INTRODUCTION

The so-called semiclassical wave-packet approach has been successfully applied to study the motion of electrons in crystals [1,2]. Most notably, in the semiclassical equations of motion (SC-EOM) for the wave packet, anomalous velocities in terms of the Berry curvatures play a key role in understanding the steady transport properties for a number of phenomena, including the anomalous Hall effect [3–7], spin Hall effect [8,9], and the valley Hall effect [10,11], as well as chiral anomaly in Weyl metals [12]. The nonsymplectic structure of the SC-EOM [13,14] also raises interest in its real-time dynamics in the context of Dirac semimetals [15] and diffusive processes [16,17]. The potential utility of the semiclassical wave-packet approach merits further attention.

In general, given the strength of the applied electric field, the bands of an electronic material can be grouped into manifolds, see Fig. 1. Those bands whose spacings are small in comparison to the energy scale associated with the external field are grouped into the same manifold. By definition, intermanifold energy spacing is much larger than the applied field. When one focuses on the motion of a wave packet within a particular manifold, the effects of other manifolds are manifested by the Berry curvatures in the SC-EOM. [2] We call the manifold of focus the active manifold and the bands within that manifold active bands. The already known semiclassical

wave packet approaches mainly deal with two situations in the active manifold. The first is that the active manifold has only one band with Abelian Berry curvatures [18–20]. The second is that it consists of several degenerate bands with non-Abelian Berry curvatures [21,22]. For both cases, given the large gaps between different manifolds, the effect of an electric field whose strength is small in comparison to these gaps can be well captured by the first-order adiabatic approximation, which accounts the electric field to the first order. However, in addition to these two situations, there is a third situation where the active manifold contains several non-degenerate bands. For this third case, although the effect of the electric field on an intermanifold transition can be accounted by the same approximation; its effect on the intramanifold transitions, due to the relatively small energy separations, should be taken into account to all orders and is expected to induce nonadiabatic dynamics. Henceforth, throughout this paper, we term this third case as nonadiabatic with the two former cases adiabatic. The purpose of the present paper is to generalize the semiclassical wave-packet approach developed in a series of studies [18–21] and reviewed in Ref. [2] for the adiabatic situation to the nonadiabatic one. This is motivated by the following realistic considerations.

(i) Berry curvature is inversely proportional to the square of the gap and therefore features a hot spot at the small gaps typically arising from band anticrossings. Examples include gapped graphene [23,24] and the recently discovered 2D MnBi₂Te₄ (with gap sizes of tens of meV) [25–28]. Electron transport under finite electric field raises the need of addressing the nonadiabaticity.

^{*}kerustemiro@gmail.com

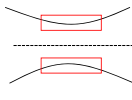
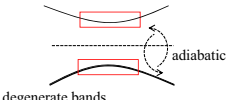
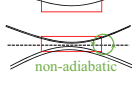
available in literatures		this work
single-band manifolds	multiple-band manifolds	
		
current Eq.(47) $J^{Ab}(\mathbf{x}) = -e \sum_n \int dk f_n \dot{x}_n$	Eq.(53) $J^{nAb} = -\frac{e^2}{\hbar} \sum_{\beta} \int dk \text{Tr}(\mathcal{F}^{k\alpha k\beta}) E_{\beta}$	Eq.(60) $\mathbf{J}(\mathbf{x}) = -e \sum_i \int dk g_i \dot{v}_i$
velocity $\dot{x}_{\alpha} = \langle [D_{\hbar k_{\alpha}}, \mathcal{H}_{\alpha}] \rangle_{\alpha} - \sum_{\beta} \left(\langle \mathcal{F}^{k_{\alpha} x \beta} \rangle_{\alpha} \dot{x}_{\beta} + \langle \mathcal{F}^{k_{\alpha} k_{\beta}} \rangle_{\alpha} \dot{k}_{\beta} \right)$ force $\hbar \dot{k}_{\alpha} = -e E_{\alpha} - \langle [D_{x_{\alpha}}, \mathcal{H}_{\alpha}] \rangle_{\alpha} + \hbar \sum_{\beta} \left(\langle \mathcal{F}^{x_{\alpha} x \beta} \rangle_{\alpha} \dot{x}_{\beta} + \langle \mathcal{F}^{x_{\alpha} k_{\beta}} \rangle_{\alpha} \dot{k}_{\beta} \right)$	Eq.(42)	Eq.(58) $\dot{v}_i = \left\langle u_i \left \frac{\partial \mathcal{H}^c}{\partial \hbar k} \right u_i \right\rangle$ $\hat{F}_i = - \left\langle u_i \left \frac{\partial \mathcal{H}^c}{\partial x} \right u_i \right\rangle$

FIG. 1. The bands are grouped into manifolds, each indicated by a red box. Inter manifold energy spacing is much larger than the applied electric field. The two left columns are the scenarios where each manifold either has a single band only or consists of fully degenerate bands. The corresponding currents are given, respectively, by Eqs. (47) and (53), which directly make use of center-of-mass SC-EOM, Eq. (42) [and its single-band reduction, Eqs. (43)]. In the rightmost column, the manifold enclosing the Fermi energy (dashed line) consists of several nondegenerate bands with small energy spacing/gap. Nonadiabatic generalization takes into account decoherence, whose joint action with driving electric field favors a certain form of interband coherence, which affects center-of-mass variables as given by Eqs. (58) and results in a current given by Eq. (60). See Sec. III for detailed discussions.

(ii) The wave-packet approach can directly address spatially varying band structures, in addition to momentum textures, exemplified by its application to systems with deformation potentials [20] and magnetic textures [29,30]. Spatially varying band structures are also relevant in long-period moiré superlattices (with periods much larger than the lattice constant) of high current interest. Experimentally, the location dependence of gap sizes has already been observed [31,32]. However, theoretical understanding of the electronic structures is mainly limited to moiré minibands [33–35], which treats the long-period moiré pattern from the perspective of global band structure and henceforth does not address explicitly the spatial textures. The wave-packet approach is, on one hand, complementary to the miniband picture and, on the other hand, beneficial when the moiré pattern is nonperiodic, as found in most experimental realities. The nonadiabatic effects are sometimes inevitable due to moiré spatial textures. Gapped graphene on hexagonal boron nitrides [23,24] is such an example, where an infinitesimal local gap exists due to sign reversal of the gap as a function of location.

Generalization of the semiclassical wave-packet approach developed in the adiabatic regime to the nonadiabatic regime is not straightforward. This can be seen from the two primary steps in constructing a semiclassical wave-packet theory for studying electron transport [1,2]. In the first step, one obtains the SC-EOM for the center of mass of a single wave packet. For the second step, one considers an electron gas as an ensemble of wave packets and computes the current \mathbf{J}

by [1,2,18,19,22]

$$\mathbf{J} = -e \int d\mathbf{k} f(\mathbf{k}) \dot{\mathbf{x}}, \quad (1)$$

where $\dot{\mathbf{x}}$ is the velocity of the wave packet obtained from the SC-EOM in the first step and $f(\mathbf{k}) = f_0(\mathbf{k}) + \delta f(\mathbf{k})$ is the carrier distribution function in which $f_0(\mathbf{k})$ is the equilibrium part and δf is the deviation from equilibrium. For the adiabatic cases, where the active manifold has only one band or degenerate bands, $f_0(\mathbf{k})$ can be unambiguously assigned by the Fermi distribution function evaluated with that particular band energy. However, in the nonadiabatic situation, the electron has interband coherence among a number of bands with distinct energies and various occupations within the active manifold. Even just evaluating the equilibrium part of the distribution function raises ambiguity. For studies involving the magnetization currents, [36,37]. Equation (1) is referred to as the local current to distinguish it from the magnetization current, which we do not discuss here.

Figure 1 tabulates available formulas as our reference for making generalizations in the first two columns. The third column summarizes the generalized results from this paper. In Sec. II A, we derive the SC-EOM of a wave packet using a different approach, without repeating the derivation by the variational approach for a wave-packet-based Lagrangian [2,18–21]. How the SC-EOM emerges from a more fundamental quantum consideration has long been interesting, within both the conventions of solid-state physics [19–22,38–45] and mathematical physics, [46–50]. Here we start from the full-band space and introduce a force operator similar to the spirit of the Ehrenfest theorem. We will show that with the aid of the Newtonian law for the time-changing rate of momentum, SC-EOM straightforwardly arises. In Sec. II B, we discuss how the Berry curvatures appear in the SC-EOM [19–21] when one groups the full bands into manifolds and focuses on a particular one. We will see that when the active manifold contains several bands, non-Abelian Berry curvatures are obtained without requiring exact degeneracy within this manifold, i.e., for the situations illustrated in the second and the third columns of Fig. 1. By definition, the non-Abelian Berry curvature reduces to an Abelian one by reducing the number of bands in the active manifold to one. In Sec. III, we turn to an ensemble of wave packets for semiclassically computing the current for an electron gas. The gas of electrons is inspected using the kinetic theory [1] and we extend it to include nonadiabatic effects by taking into account decoherence, whose joint action with the electric field favors a certain form of interband coherence. We then show the reproduction of known results by reducing the active manifold to contain either one band or only degenerate bands. A summary is in Sec. IV.

II. SEMICLASSICAL WAVE-PACKET DYNAMICS

In this section, we first concentrate on the dynamics of a single wave packet in a system of multiple bands with spatially varying band structures. In the series of works on the adiabatic wave-packet theory [18–21], one can identify a main theoretical framework and over this main framework two “corrections” can be considered, namely, the gradient

correction[20] and the correction to the density of states in the phase space [13]. To concentrate on the nonadiabatic issue arising from narrow gaps under finite electric field, we ignore both of these two corrections here. Therefore, the present theory is only restricted to the cases of very smooth spatial variations such that the gradient correction is expected to be insignificant. We also exclusively consider transport driven only by an external electric field and we assume that there is no external magnetic field. As we will show later in Sec. III, the known density of states correction involves a particular feature of the adiabatic wave-packet dynamics which is no longer available in the nonadiabatic regime.

A. Full-band dynamics of an electron wave packet in spatial and momentum textures

Spatially varying band structures can be obtained by designing to each local region a Hamiltonian with corresponding periodic potential. This so-called local Hamiltonian can be understood as the Hamiltonian experienced by an electron localized as a wave packet in the corresponding region, with the capacity to encode the information of spatial textures [20–22]. The real-space coordinate \mathbf{x}_c of the wave packet's center parameterizes and characterizes such a local Hamiltonian, denoted as $H_c(\mathbf{x}_c, t)$, where the extra time dependence t comes from a time-dependent vector potential.

The local Hamiltonian possesses Bloch states as its eigenstates denoted by $|\psi_{n,q}(\mathbf{x}_c, t)\rangle$ with eigenenergies $\varepsilon_{n,q}(\mathbf{x}_c, t)$ where n is the band index, \mathbf{q} is the momentum quantum number, and (\mathbf{x}_c, t) reminds us of the parameterization of the local Hamiltonian. This guarantees that the corresponding Schrödinger equation,

$$H_c(\mathbf{x}_c, t)|\Phi(t)\rangle = i\hbar|\dot{\Phi}(t)\rangle, \quad (2)$$

has a solution of the form

$$|\Phi(t)\rangle = \sum_n \eta_n(t)|\psi_{n,q_c}(\mathbf{x}_c, t)\rangle. \quad (3)$$

In principle, the wave function in a slowly perturbed crystal is a continuous superposition of Bloch states that has a certain extension in momentum space and consequently also has a width in real space, thus pictured as a wave packet. The size of the wave packet is large compared to the lattice constant of the local crystalline structure and small compared to the length scale over which the local crystalline structure smoothly varies and its extension in momentum space is sharply centered at some momentum \mathbf{q}_c . We then approximate the wave function by Eq. (3) and understand it as a wave packet parameterized by the real-space center \mathbf{x}_c and the momentum-space center $\hbar\mathbf{q}_c$, namely, $|\Phi(t)\rangle = |\Phi(\mathbf{q}_c, \mathbf{x}_c, t)\rangle$. Note here that in Eq. (3), the band index n is summed over all bands of $H_c(\mathbf{x}_c, t)$ for the proper inclusion of nonadiabatic effects.

As the wave packet can move throughout the space, its position \mathbf{x}_c and momentum $\hbar\mathbf{q}_c$ can change over time. The changing rate $\dot{\mathbf{x}}_c$ is naturally the velocity and $\hbar\dot{\mathbf{q}}_c$ is interpreted as the force associated with the rate of change of the crystal momentum. Using the Heisenberg EOM, the velocity operator is found to be

$$\hat{V}(\mathbf{x}_c, t) = -\frac{i}{\hbar}[\hat{X}, H_c(\mathbf{x}_c, t)], \quad (4)$$

The expectation value of the velocity operator should be the wave packet's spatial velocity,

$$\dot{\mathbf{x}}_c = \langle\Phi(t)|\hat{V}(\mathbf{x}_c, t)|\Phi(t)\rangle, \quad (5)$$

on a self-consistent ground.

In the Ehrenfest theorem, the so-called force operator is defined by the minus of the potential gradient. Similarly, here we define a force operator by

$$\hat{F}(\mathbf{x}_c, t) = -\frac{\partial H_c(\mathbf{x}_c, t)}{\partial \mathbf{x}_c}. \quad (6)$$

The expectation value of the Ehrenfest's force operator gives the time derivative of the expectation value of the bare momentum operator. In parallel to this, we replace the bare momentum by the crystal momentum $\hbar\mathbf{q}_c$ in our case, and its time derivative is then assumed to be the expectation value of the corresponding force operator, namely,

$$\hbar\dot{\mathbf{q}}_c = \langle\Phi(t)|\hat{F}(\mathbf{x}_c, t)|\Phi(t)\rangle. \quad (7)$$

Substituting Eq. (3) into Eqs. (5) and (7), we are led to

$$\dot{\mathbf{x}}_c = \langle\chi(t)|\frac{\partial \mathcal{H}^c(\mathbf{x}_c, \mathbf{q}_c, t)}{\partial \hbar\mathbf{q}_c}|\chi(t)\rangle, \quad (8)$$

$$\hbar\dot{\mathbf{q}}_c = -\langle\chi(t)|\frac{\partial \mathcal{H}^c(\mathbf{x}_c, \mathbf{q}_c, t)}{\partial \mathbf{x}_c}|\chi(t)\rangle, \quad (9)$$

where $\mathcal{H}^c(\mathbf{x}_c, \mathbf{q}_c, t) = e^{-iq_c \cdot \hat{X}} H_c(\mathbf{x}_c, t) e^{iq_c \cdot \hat{X}}$. Here $|\chi(t)\rangle = \sum_n \eta_n(t)|u_{n,q_c}(\mathbf{x}_c, t)\rangle$ with $|u_{n,q_c}(\mathbf{x}_c, t)\rangle = e^{-iq_c \cdot \hat{X}} |\psi_{n,q_c}(\mathbf{x}_c, t)\rangle$ and is subject to

$$\mathcal{H}^c(\mathbf{x}_c, \mathbf{q}_c, t)|\chi(t)\rangle = i\hbar|\dot{\chi}(t)\rangle. \quad (10)$$

The set of SC-EOM, Eqs. (8) and (9), for the wave packet's center-of-mass $(\mathbf{x}_c, \hbar\mathbf{q}_c)$ are coupled to the quantum Schrödinger equation, Eq. (10), which describes superposition among bands by the state vector, $|\chi\rangle$, quantified by the band amplitudes η_n 's. The physical state of the wave packet is thus completely specified by its center-of-mass $(\mathbf{x}_c, \hbar\mathbf{k}_c)$ plus $|\chi\rangle$, here called the band state. We will show how Eqs. (8) and (9) can be recast into the more familiar gauge-covariant form Eqs. (14) and (15) in Sec. II A 1.

The wave packet's velocity, Eq. (8), can be decomposed in the band basis as

$$\dot{\mathbf{x}}_c = \mathbf{v}_b + \mathbf{v}_h, \quad (11a)$$

where

$$\mathbf{v}_b \equiv \sum_n \eta_n^* \langle u_n | \frac{\partial \mathcal{H}^c}{\partial \hbar\mathbf{q}_c} | u_n \rangle \eta_n = \sum_n |\eta_n|^2 \frac{\partial \varepsilon_n}{\partial \hbar\mathbf{q}_c} \quad (11b)$$

is the normal velocity associated with the dispersion of each band and

$$\mathbf{v}_h \equiv \sum_n \sum_{m \neq n} \eta_n^* \langle u_n | \frac{\partial \mathcal{H}^c}{\partial \hbar\mathbf{q}_c} | u_m \rangle \eta_m \quad (11c)$$

is the anomalous velocity which is eventually expressed in terms of Berry curvatures when we group bands into manifolds (see later discussion). Here we have abbreviated $|u_n\rangle$ for $|u_{n,q_c}(\mathbf{x}_c, t)\rangle$ and ε_n for $\varepsilon_{n,q_c}(\mathbf{x}_c, t)$, respectively.

Assuming initially that the electron only occupies one particular band n_0 , namely, $\eta_n(t_0) = \delta_{n,n_0}$, the system described

by Eq. (2) [and, consequently, by Eqs. (8)–(10)] under no external field will remain in just occupying that band n_0 , rendering $\eta_n(t) = 0$ whenever $n \neq n_0$. In such a trivial situation, the anomalous velocity \mathbf{v}_h would be zero. The anomalous motion, in contrast to the normal one, is thus a result of interband transitions induced by the external field. In addition, for transitions between a pair of degenerate bands (n, m) with $n \neq m$ and $\varepsilon_n = \varepsilon_m \equiv \varepsilon^d$, we have in general

$$\langle u_n | \frac{\partial \mathcal{H}^c}{\partial \hbar \mathbf{q}_c} | u_m \rangle = \varepsilon^d \frac{\partial}{\partial \mathbf{q}_c} \langle u_n | u_m \rangle = \varepsilon^d \frac{\partial \delta_{n,m}}{\partial \mathbf{q}_c} = 0. \quad (12)$$

Only transitions between nondegenerate bands in Eq. (11c) contribute to the anomalous velocity.

1. Gauge invariance of expectation values of observables and gauge covariance form of EOM

In principle, the motion of a wave packet in multiple bands can be studied using Eqs. (8)–(10). To verify their validity, we will connect them with the more familiar form of SC-EOM [19–21] in which the Berry curvatures explicitly appear. First, we define the Berry connections,

$$[\mathcal{R}_{\lambda_\alpha}]_{n,m} = \left\langle u_n \left| i \frac{\partial u_m}{\partial \lambda_\alpha} \right. \right\rangle, \quad (13)$$

in the phase space $\boldsymbol{\lambda} = (\mathbf{x}_c, \hbar \mathbf{q}_c)$, where λ_α stands for the α th component of $\boldsymbol{\lambda}$. Using the decomposition Eqs. (11) with the observation, $\sum_n \sum_{m \neq n} \eta_n^* \langle u_n | i \frac{\partial \mathcal{H}^c}{\partial \hbar \mathbf{q}_c} | u_m \rangle \eta_m = -i \sum_n \sum_{m \neq n} \eta_n^* [\mathcal{R}_{\hbar \mathbf{q}_c}, \mathcal{H}^c]_{n,m} \eta_m$, and applying similar decomposition to Eq. (9), then Eqs. (8)–(10) are rewritten into

$$\dot{\mathbf{x}}_c = \langle [\mathcal{D}_{\hbar \mathbf{q}_c}, \mathcal{H}^c] \rangle, \quad (14)$$

$$\hbar \dot{\mathbf{q}}_c = -\langle [\mathcal{D}_{\mathbf{x}_c}, \mathcal{H}^c] \rangle, \quad (15)$$

and

$$i \hbar \frac{D}{Dt} \boldsymbol{\eta}(t) = \mathcal{H}^c(t) \boldsymbol{\eta}(t), \quad (16)$$

respectively, where

$$[\mathcal{D}_{\lambda_\alpha}]_{n,m} = \delta_{n,m} \frac{\partial}{\partial \lambda_\alpha} - i [\mathcal{R}_{\lambda_\alpha}]_{n,m}, \quad (17)$$

$$\left[\frac{D}{Dt} \right]_{n,m} = \delta_{n,m} \frac{d}{dt} - i \sum_\alpha [\mathcal{R}_{\lambda_\alpha}]_{n,m} \dot{\lambda}_\alpha, \quad (18)$$

Here $\langle O \rangle = \sum_{n,m} \eta_n^* O_{n,m} \eta_m$ for any matrix quantity O and $\boldsymbol{\eta}$ the column vector with entries η_n 's. The expression Eq. (14) bares the interpretation of gauge covariant group velocity [21] due to the appearance of the so-called covariant derivative, Eq. (17). From the above derivations, we see that this gauge covariant group velocity Eq. (14) is exactly the expectation value of the quantum velocity operator under the dynamics of the wave packet's local Hamiltonian, Eq. (8). The equality between Eqs. (14) and (8) and the equality between Eqs. (15) and (9) simply manifest the gauge invariance of the expectation values of physical observables described by gauge-covariant EOM.

The more familiar form of Eq. (15) or Eq. (9) explicitly contains a term proportional to the external electric field $\mathbf{E}(\mathbf{x}_c, t) = -\partial \mathbf{A} / \partial t - \partial \delta \phi / \partial \mathbf{x}_c$, where $\delta \phi$ is the externally

applied scalar potential that smoothly changes in space. This is easily arrived at by the translational invariance that relates the Bloch state for momentum $\hbar \mathbf{q}_c$ via the vector potential \mathbf{A} to $\hbar \mathbf{k}_c$ by $\hbar \mathbf{k}_c = \hbar \mathbf{q}_c - (-e)\mathbf{A}$ in which $\hbar \mathbf{k}_c$ is called mechanical crystal momentum [20]. We further replace $\partial / \partial \mathbf{q}_c$ appearing in $\dot{\mathbf{x}}_c$ by $\partial / \partial \mathbf{k}_c$ according to the chain rule, resulting in [51]

$$\dot{\mathbf{x}}_c = \langle [\mathcal{D}_{\hbar \mathbf{k}_c}, \mathcal{H}^c] \rangle = \langle \chi | \frac{\partial \mathcal{H}^c}{\partial \hbar \mathbf{k}_c} | \chi \rangle \quad (19)$$

and

$$\hbar \dot{\mathbf{k}}_c = (-e)\mathbf{E} - \langle [\mathcal{D}_{\mathbf{x}_c}, \mathcal{H}^c] \rangle = (-e)\mathbf{E} + \mathbf{F}_c, \quad (20)$$

where

$$\mathbf{F}_c = -\langle \chi | \frac{\partial \mathcal{H}^c}{\partial \mathbf{x}_c} | \chi \rangle \quad (21)$$

and \mathcal{H}^c in Eqs. (19) and (20) is

$$\mathcal{H}^c(\mathbf{x}_c, \mathbf{k}_c) = e^{-i\mathbf{k}_c \cdot \hat{\mathbf{X}}} H_c(\mathbf{x}_c, t) |_{A=0, \delta \phi=0} e^{i\mathbf{k}_c \cdot \hat{\mathbf{X}}}, \quad (22)$$

and does not explicitly depend on t since the explicit t dependence in $H_c(\mathbf{x}_c, t)$ solely comes from the electric-field-generating vector potential. Note that the trivial case of spatial variations in which all bands' energies change by the same amount in space has already been taken care of by $\delta \phi$ so \mathbf{E} can be dependent on \mathbf{x}_c .

In the ideal case of no spatial perturbation, as for what occurs in a perfect periodic lattice without electromagnetic field, the local Schrödinger equation becomes globally valid and $\partial H_c(\mathbf{x}_c, t) / \partial \mathbf{x}_c = 0$. The description by Eq. (2) becomes a standard quantum mechanics problem for a particle moving in a periodic potential. Nevertheless, the velocity observable is still well-defined by the operator Eq. (4). The system that starts with a momentum $\hbar \mathbf{q}_c$ as a delocalized Bloch state will remain delocalized with the velocity given by the right-hand sides of Eq. (8) and equally by Eq. (14) but without the semiclassical notion as a localized wave packet.

B. Dynamics of a wave packet within the active manifold

Equations (14) and (15) already resemble the non-Abelian SC-EOM used in Refs. [2,21]. For pedagogical reasons, below we continue to discuss how the Berry curvatures emerge from Eqs. (14) and (15) or equivalently from Eqs. (8) and (9).

We denote the active manifold by a and the rest by r . With these labels of the bands, we can compactly rewrite Eqs. (14) and (15) into

$$\dot{\lambda}_\alpha = \text{sgn}(\lambda_\alpha) \left\{ \langle [\mathcal{D}_{\hat{\lambda}_\alpha}, \mathcal{H}^c_a] \rangle_a + \langle [\mathcal{D}_{\hat{\lambda}_\alpha}, \mathcal{H}^c_r] \rangle_r + \left(\sum_{n \in a} \sum_{l \in r} \eta_n^* \langle u_n | \frac{\partial \mathcal{H}^c}{\partial \hat{\lambda}_\alpha} | u_l \rangle \eta_l + \text{c.c.} \right) \right\}, \quad (23)$$

where λ_α is the α th component (in terms of spatial direction) of \mathbf{x}_c or $\hbar \mathbf{q}_c$, $\hat{\lambda}_\alpha$ stands for the conjugate, namely, $\hat{\mathbf{x}}_c = \hbar \mathbf{q}_c$ and $\hbar \hat{\mathbf{q}}_c = \mathbf{x}_c$, and the sign function values as $\text{sign}(\mathbf{x}_c) = 1$ and $\text{sign}(\hbar \mathbf{q}_c) = -1$. We use the notation $\langle O \rangle_{a/r}$ for averages only over the bands in the manifold a/r and $\mathcal{H}^c_{a/r}$ for the block of \mathcal{H}^c in the space of a/r .

The reliability of the following approximations underlie the meaning of grouping the bands into a and r [52,53]. (i) The occupation of r bands is negligible, corresponding to ignore the term $\langle \{ \mathcal{D}_{\lambda_a}, \mathcal{H}_r^c \} \rangle_r$ of Eq. (23). (ii) The coherence between a and r , described by the second line of Eq. (23) shall be kept up to the lowest order of the external field. So, leading-order effects of r on a survive. Note that the effect of the external field on transitions within the active manifold is kept to all orders.

After these approximations, Eq. (23) is then turned into Eq. (42) with the Berry curvature defined in Eq. (41) (see the derivation in the following).

1. Emergence of Berry curvatures

To see how Berry curvatures arise in the second line of Eq. (23), we have to investigate the coherent dynamics of $\eta(t)$, under an electric field which is relatively small with respect to intermanifold energy separation. Note that the coherence between bands n and m is characterized by the relative phase, $\arg(\eta_n^* \eta_m / |\eta_n^* \eta_m|)$. Naively solving Eq. (16) leads to gauge-dependent relative phases [54]. This complication is avoided by reinspecting Eq. (10) with $|\chi\rangle = \sum_n \tilde{\eta}_n |\bar{u}_n\rangle$, where

$$|\bar{u}_n\rangle = e^{i\gamma_n} |u_n\rangle \quad (24a)$$

and

$$\tilde{\eta}_n = e^{-i\gamma_n} \eta_n, \quad (24b)$$

in which γ_n is the Berry phase defined by

$$\gamma_n = \int_{(\mathbf{x}_0, \mathbf{k}_0)}^{(\mathbf{x}_c, \mathbf{k}_c)} \{ d\mathbf{x}' \cdot [\mathcal{R}_{\mathbf{x}'}]_{n,n} + d\mathbf{k}' \cdot [\mathcal{R}_{\mathbf{k}'}]_{n,n} \}. \quad (25)$$

Here $(\mathbf{x}_0, \mathbf{k}_0)$ denotes the initial value of the wave packet's center of mass. This results in

$$\tilde{\mathcal{H}}\tilde{\eta} = i\hbar\dot{\tilde{\eta}}, \quad (26)$$

where $\tilde{\eta}$ denotes the vector with entries $\tilde{\eta}_n$'s and the matrix $\tilde{\mathcal{H}}$ has elements

$$\tilde{\mathcal{H}}_{n,m} = \delta_{n,m}\varepsilon_n + (1 - \delta_{n,m})V_{n,m}, \quad (27)$$

with

$$V_{n,m} = -\hbar\{ [\bar{\mathcal{R}}_{\mathbf{x}_c}]_{n,m} \cdot \dot{\mathbf{x}}_c + [\bar{\mathcal{R}}_{\mathbf{k}_c}]_{n,m} \cdot \dot{\mathbf{k}}_c \}, \quad (28)$$

in which $[\bar{\mathcal{R}}_{\mathbf{x}_c}]_{n,m} = e^{-i\gamma_n} [\mathcal{R}_{\mathbf{x}_c}]_{n,m} e^{i\gamma_m}$ with a similar definition applied to $[\bar{\mathcal{R}}_{\mathbf{k}_c}]_{n,m}$. Here $\tilde{\mathcal{H}}$ is effectively a Hamiltonian in the moving frame of the carrier, whose motion in the phase space due to the electric field and the spatial variation of the band structures induces interband coherent hybridization, mediated by the matrix elements with $n \neq m$ in Eq. (27) [55].

We denote the projection of $\tilde{\eta}$ on the a bands by $\tilde{\eta}_a$ and those on r by $\tilde{\eta}_r$, namely, $\tilde{\eta} = \begin{pmatrix} \tilde{\eta}_a \\ \tilde{\eta}_r \end{pmatrix}$, and Eq. (26) becomes

$$\begin{pmatrix} \tilde{\mathcal{H}}_a & V_{a,r} \\ V_{r,a} & \tilde{\mathcal{H}}_r \end{pmatrix} \begin{pmatrix} \tilde{\eta}_a \\ \tilde{\eta}_r \end{pmatrix} = i\hbar \begin{pmatrix} \dot{\tilde{\eta}}_a \\ \dot{\tilde{\eta}}_r \end{pmatrix}, \quad (29)$$

where $\tilde{\mathcal{H}}_a$ ($\tilde{\mathcal{H}}_r$) is the a (r) block of the effective Hamiltonian $\tilde{\mathcal{H}}$ in Eq. (27) and $V_{a,r} = -\hbar\tilde{\mathcal{K}}^{a,r}$ with $[\tilde{\mathcal{K}}^{a,r}]_{n,l} \equiv \{ [\bar{\mathcal{R}}_{\mathbf{x}_c}]_{n,l} \cdot \dot{\mathbf{x}}_c + [\bar{\mathcal{R}}_{\mathbf{k}_c}]_{n,l} \cdot \dot{\mathbf{k}}_c \}$ for $n \in a$ and $l \in r$ with $V_{r,a} =$

$-\hbar\tilde{\mathcal{K}}^{r,a}$ the Hermitian conjugate of $V_{a,r}$. It is convenient to work in the rotating frame by defining

$$\tilde{\eta}(t) = U_0^\dagger(t)\tilde{\eta}(t), \quad (30)$$

where

$$U_0(t) = \begin{pmatrix} U_a(t) & 0 \\ 0 & U_r(t) \end{pmatrix}, \quad (31)$$

with $U_{a/r}(t) = \hat{T} \exp \{ -\frac{i}{\hbar} \int_{t_0}^t d\tau \tilde{\mathcal{H}}_{a/r}(\tau) \}$ in which \hat{T} is the time-ordering operator and t_0 is the initial time. Since the strength of the coupling $V_{a,r}$ is inversely proportional to the large energy separation between a and r , it is treated as a perturbation. Up to the leading order, we have

$$\dot{\tilde{\eta}}(t) \approx i\tilde{\mathcal{K}}_{\text{mix}}\tilde{\eta}(t_0), \quad (32)$$

where

$$\tilde{\mathcal{K}}_{\text{mix}} = \begin{pmatrix} 0 & U_a^\dagger \tilde{\mathcal{K}}^{a,r} U_r \\ U_r^\dagger \tilde{\mathcal{K}}^{r,a} U_a & 0 \end{pmatrix}. \quad (33)$$

We assume initially there is no occupation on r bands, namely, $\tilde{\eta}_r(t_0) = 0$. This initial condition together with the approximation Eq. (32) results in

$$i\hbar\dot{\tilde{\eta}}_a = \tilde{\mathcal{H}}_a \tilde{\eta}_a, \quad (34)$$

which describes the coherent dynamics of the band amplitudes within the active manifold, also called the *band pseudospin*. We are interested only in the interband transitions among the bands in a and we neglect the interband transitions among the bands in r , leading to

$$\dot{\tilde{\eta}}_{l \in r} = i \sum_{m \in a} e^{(i/\hbar) \int_{t_0}^t ds (\varepsilon_l(s) - \varepsilon_m(s))} [\tilde{\mathcal{K}}^{r,a}]_{lm} \tilde{\eta}_m. \quad (35)$$

Due to the large gap, the exponential factor oscillates very fast while the adiabatic approximation gives that the intermanifold coupling $[\tilde{\mathcal{K}}^{r,a}]_{lm}$ changes slowly. Following the adiabatic approximations in Ref. [2], we can perform integration by parts on Eq. (35), yielding

$$\tilde{\eta}_l = \sum_{m \in a} \frac{\hbar [\tilde{\mathcal{K}}^{r,a}]_{lm}}{(\varepsilon_l - \varepsilon_m)} \tilde{\eta}_m. \quad (36)$$

Defining the dimensionless factors,

$$\epsilon = \left| \frac{\hbar [\tilde{\mathcal{K}}^{r,a}]_{lm}}{(\varepsilon_l - \varepsilon_m)} \right|, \quad (37)$$

we see the average on the r bands, $\langle \{ \mathcal{D}_{\lambda_a}, \mathcal{H}_r^c \} \rangle_r$, is two orders of ϵ smaller than $\langle \{ \mathcal{D}_{\lambda_a}, \mathcal{H}_a^c \} \rangle_a$ and the occupations on the r bands are thus neglected. Substituting Eq. (36) into Eq. (23) with the aid of Eqs. (24), the contribution from transitions between a and r to the velocity $\dot{\mathbf{x}}_c$ reads

$$\begin{aligned} & \left(\sum_{n \in a} \sum_{l \in r} \eta_n^* \langle u_n | \frac{\partial \mathcal{H}^c}{\partial \lambda_\alpha} | u_l \rangle \eta_l + \text{c.c.} \right) \\ &= -i\hbar \sum_{\beta} \sum_{n \in a} \sum_{l \in r} \eta_n^* \sum_{m \in a} \frac{(\varepsilon_l - \varepsilon_n)}{(\varepsilon_l - \varepsilon_m)} \\ & \times \left\langle \frac{\partial u_n}{\partial \lambda_\alpha} \middle| u_l \right\rangle \left\langle u_l \middle| \frac{\partial u_m}{\partial \lambda_\beta} \right\rangle \dot{\lambda}_\beta \eta_m + \text{c.c.}, \quad (38) \end{aligned}$$

where $\hat{\lambda}_\alpha$ is the α th component of $\hbar\mathbf{k}_c$. The same expression applies to the contribution from the a - r transition to the force $\hbar\dot{\mathbf{k}}_c$ with $\hat{\lambda}_\alpha$ replaced by the α th component of \mathbf{x}_c . The remoteness of bands in r from a assures the validity of the approximation,

$$\frac{(\varepsilon_l - \varepsilon_n)}{(\varepsilon_l - \varepsilon_m)} \approx 1, \quad (39)$$

without requiring exact degeneracy among the bands in a . Furthermore, we observe that

$$i \left\{ \left\langle \frac{\partial u_n}{\partial \hat{\lambda}_\alpha} \left[\sum_{l \in r} |u_l\rangle \langle u_l| \right] \frac{\partial u_m}{\partial \lambda_\beta} \right\rangle - (\lambda_\beta \leftrightarrow \hat{\lambda}_\alpha) \right\} = \mathcal{F}_{nm}^{\hat{\lambda}_\alpha \lambda_\beta} \quad (40)$$

is the non-Abelian Berry curvature matrix that can be rewritten in a more familiar form,

$$\mathcal{F}_{nm}^{\hat{\lambda}_\alpha \lambda_\beta} = \left\{ \frac{\partial [\mathcal{R}_{\lambda_\beta}]_{nm}}{\partial \hat{\lambda}_\alpha} - \frac{\partial [\mathcal{R}_{\hat{\lambda}_\alpha}]_{nm}}{\partial \lambda_\beta} - i[\mathcal{R}_{\hat{\lambda}_\alpha}, \mathcal{R}_{\lambda_\beta}]_{nm} \right\}, \quad (41)$$

with the help of Eq. (13). Using the approximation Eq. (39) in Eq. (38) for Eq. (23) with the identification of Eq. (40) with Eq. (41), we finally see that Eqs. (8) and (9) or equivalently Eqs. (14) and (15) [summarized as Eq. (23)] reduce to the non-Abelian SC-EOM in Ref. [21], namely,

$$\dot{x}_\alpha = \langle [\mathcal{D}_{\hbar\mathbf{k}_\alpha}, \mathcal{H}_a^c] \rangle_a - \sum_\beta (\langle \mathcal{F}^{k_\alpha x_\beta} \rangle_a \dot{x}_\beta + \langle \mathcal{F}^{k_\alpha k_\beta} \rangle_a \dot{k}_\beta), \quad (42a)$$

$$\hbar\dot{k}_\alpha = -eE_\alpha - \langle [\mathcal{D}_{x_\alpha}, \mathcal{H}_a^c] \rangle_a + \hbar \sum_\beta (\langle \mathcal{F}^{x_\alpha x_\beta} \rangle_a \dot{x}_\beta + \langle \mathcal{F}^{x_\alpha k_\beta} \rangle_a \dot{k}_\beta). \quad (42b)$$

We have omitted the subscript c for the center-of-mass variables, writing $(x_{c\alpha}, k_{c\alpha})$ simply by (x_α, k_α) .

We thus have deduced the SC-EOM with explicit appearance of Berry curvatures, Eq. (42), in a proper limit from the full-band dynamics, namely, Eqs. (8) and (9), or compactly as Eq. (23). The Abelian formulation [19,20] is obtained from Eq. (42) by letting the manifold a contain only one band, resulting in

$$\dot{x}_\alpha = \frac{\partial \varepsilon_n}{\partial \hbar k_\alpha} - \sum_\beta (\Omega_n^{k_\alpha x_\beta} \dot{x}_\beta + \Omega_n^{k_\alpha k_\beta} \dot{k}_\beta), \quad (43a)$$

$$\hbar\dot{k}_\alpha = -eE_\alpha - \frac{\partial \varepsilon_n}{\partial x_\alpha} + \hbar \sum_\beta (\Omega_n^{x_\alpha x_\beta} \dot{x}_\beta + \Omega_n^{x_\alpha k_\beta} \dot{k}_\beta), \quad (43b)$$

where

$$\Omega_n^{\lambda_\alpha \lambda_\beta} = \frac{\partial [\mathcal{R}_{\lambda_\beta}]_{nn}}{\partial \lambda_\alpha} - \frac{\partial [\mathcal{R}_{\lambda_\alpha}]_{nn}}{\partial \lambda_\beta} \quad (44)$$

is the Abelian Berry curvature for the band indexed by n . The second terms in Eqs. (42) and (43) in terms of the Berry curvatures are of $\mathcal{O}(\epsilon)$, where ϵ is defined by Eq. (37).

2. Nonadiabaticity within the active manifold

The SC-EOM, Eq. (42), for the wave-packet dynamics within the active manifold already cover both the adiabatic (single band or several degenerate bands) and the nonadiabatic (several nondegenerate bands) cases, including effects from

the momentum as well as the spatial textures. Degeneracy among active bands brings forth $U(N)$ symmetry, where N is the number of bands within the active manifold and enables formal connection to non-Abelian gauge structure [56]. The second term of Eq. (42) as the non-Abelian curvature has been a focus of previous discussions [2,21,22]. To relate wave-packet dynamics to geometric effects arising from closed trajectories over the phase space with $U(N)$ symmetry, keeping degeneracy along the trajectories is thus presumed [56]. Note that Eq. (42) makes no strict restrictions on energy spacing among the active bands over the phase space as long as they are far enough separated from r bands for Eq. (39) to be a good approximation.

Here we want to address the first term of Eq. (42) that contains nonadiabatic effects within the active manifold. Interestingly, from Eqs. (11) and (12), degeneracy makes zero contributions to the anomalous velocity. Nonzero contribution to v_n only comes from intermanifold transitions, as the second term of Eq. (42), and crucially intra-manifold transitions among nondegenerate active bands, embedded in the first term of Eq. (42). Recall from Sec. II B 1 that the emergence of the second term of Eq. (42) as non-Abelian Berry curvatures is from a perturbation correction to the first order of a small parameter, ϵ , Eq. (37). Its contribution is thus on the order $\mathcal{O}(\epsilon)$. In contrast, the first term of Eq. (42) that incorporates nonadiabatic effects is on the order of ϵ^0 . The consequence of this difference between adiabatic and nonadiabatic dynamics for multiple active bands on the current will be further explored in Sec. III C.

A number of physical realizations exists for manifesting the importance of the nonadiabatic dynamics. This includes materials with narrow band gaps whose sizes are comparable to the electric field, for example, those featuring band anticrossings such as gapped Dirac cones [9,25–28] and gap sign reversal in moiré patterns [23,24]. Although the form of Eq. (42) has already appeared in the literature, the implications of the nonadiabatic contents of such EOM for a single wave packet have not been fully explored in terms of the current for an ensemble of wave packets. Below, we continue to discuss the steady-state transport within the semiclassical picture. We assume the electric field no longer changes with time in the steady-state limit.

III. SEMICLASSICAL TRANSPORT THEORIES

A semiclassical transport theory is featured by the capability of calculating the current within the phase-space framework for an ensemble of electron wave packets forming an electron gas. The single-wave-packet basis for the description of the ensemble is the SC-EOM. Each manifold has its corresponding SC-EOM. Summing over contributions from the relevant manifolds (e.g., the lowest conduction band and the top valence band, in the case of a large gap semiconductor) then gives the current for the ensemble.

A well-established semiclassical transport theory is the standard kinetic theory [1], which relies on the availability of single-band manifolds with the SC-EOM given by Eqs. (43). The expression for the current is the familiar form, Eq. (47) (see details in Sec. III A 2). This well-established transport theory based on single-band manifolds is referred to here as

single-band semiclassical transport theory (SSCT). For being self-content, we first review in Sec. III A the known results of SSCT and its correspondence to the pure classical picture of a phase-space fluid (PSF). The original picture of PSF is important in understanding the semiclassical current in SSCT.

When one relevant manifold consists of multiple bands, the corresponding SC-EOM is given by Eq. (42), regardless of it is degenerate or not. The transport theory for such multiple-band manifold is referred to here as multiple-band semiclassical transport theory (MSCT). In Sec. III B, we first show that the nature of having multiple bands, regardless of being degenerate or not, renders it difficult to directly extend from SSCT to MSCT. Nevertheless, under restricted conditions (see Sec. III B 3 for details), straightforward generalization from SSCT to MSCT results in a familiar expression of current, Eq. (53), in terms of non-Abelian Berry curvatures. With these preparations, in Sec. III C, we devise a theory for MSCT including nonadiabatic effects for evaluating the current within the phase-space framework.

A. Semiclassical transport theory and the PSF

1. Fundamental elements of classical PSF

In the classical analysis of the particle transport, we rely on the picture of a mass of fluid distributed in the phase space, the so-called PSF. The PSF is characterized by two ingredients. One ingredient is the mass distribution $f(\mathbf{x}, \hbar\mathbf{k})$ and the other is the fluid's velocity distribution $\mathcal{V}(\mathbf{x}, \hbar\mathbf{k})$. The former specifies the amount of the PSF's mass occupying an elemental area of the phase space centered around $(\mathbf{x}, \hbar\mathbf{k})$. The latter $\mathcal{V}(\mathbf{x}, \hbar\mathbf{k}) = (\dot{\mathbf{x}}, \hbar\dot{\mathbf{k}})$ has a position component $\dot{\mathbf{x}}$ and a momentum component $\hbar\dot{\mathbf{k}}$. The PSF's velocity are specified by the EOM for a single particle. The particle current density $\mathbf{J}(\mathbf{x})$ at real-space position \mathbf{x} is given by

$$\mathbf{J}^{\text{cl}}(\mathbf{x}) = \int d\mathbf{k} f(\mathbf{x}, \hbar\mathbf{k}) \mathbf{v}(\mathbf{x}, \hbar\mathbf{k}), \quad (45)$$

where $\mathbf{v}(\mathbf{x}, \hbar\mathbf{k}) = \dot{\mathbf{x}}$ is built from the single-particle dynamics.

There is an important property of the classical transport theory that is to be inherited to a semiclassical construction which enables the description of the current for an electron gas. This property is that the fluid's mass distribution $f(\mathbf{x}, \hbar\mathbf{k})$ and velocity distribution $\mathcal{V}(\mathbf{x}, \hbar\mathbf{k})$ are both completely determined by the phase-space coordinate $(\mathbf{x}, \hbar\mathbf{k})$. The former is an inherited part of the definition of a phase space. The latter is ensured by the nature of the classical Hamiltonian dynamics. This property is called the phase-space locality.

In summary, there are two fundamental elements in a classical transport theory. (i): The single-particle's EOM satisfies the phase-space locality. (ii) There exists a nonambiguous distinction between the PSF's mass and velocity distributions. The velocity distribution is directly based on the scattering-free single-particle dynamics while the scattering-induced effects are included only through the mass distribution $f(\mathbf{x}, \hbar\mathbf{k})$. Note that in the semiclassical treatment of the anomalous Hall effect, the so-called side-jump velocity involves averaging over scattering [57]. Here we do not discuss the side-jump effects.

2. The correspondence between PSF and SSCT

Here we discuss how the above fundamental elements of classical transport theory are preserved in the SSCT.

(i) The restriction of having only a single band in the active manifold lets the SC-EOM, Eqs. (43), exhibit the phase-space locality. However, the phase-space locality is not guaranteed in Eq. (42) (see discussions in Sec. III B). Henceforth, a sufficiently small external field that enables one to focus on a single band at a time is vital to the phase-space locality.

(ii) Being able to focus at a time on a single-band manifold, indexed by its band n , also furnishes the specification of the PSF's mass for that band by associating it with an equilibrium Fermi-Dirac distribution f_n^0 and a nonequilibrium deviation δf_n , namely,

$$f_n = f_n^0 + \delta f_n, \quad (46a)$$

in which

$$f_n^0 = \frac{1}{e^{(\varepsilon_n - \mu)/k_B T} + 1}, \quad (46b)$$

with the chemical potential μ , the temperature T , and Boltzmann constant k_B . Under the widely applied relaxation-time approximation [18,19,58–60], the deviation from equilibrium reads

$$\delta f_n = -\tau \left[\frac{\partial f_n^0}{\partial \mathbf{x}} \cdot \dot{\mathbf{x}}_n + \frac{\partial f_n^0}{\partial \mathbf{k}} \cdot \dot{\mathbf{k}}_n \right], \quad (46c)$$

where τ is the scattering time. Here $(\dot{\mathbf{x}}_n, \hbar\dot{\mathbf{k}}_n)$ is given by Eqs. (43), corresponding to the PSF's velocity which is decoupled from the scattering effects. The scattering effects are incorporated only in δf_n . Therefore, the SSCT expressed by Eqs. (43) and (46) satisfies the property that the PSF's velocity and mass are well-separated notions.

For the current, the classical formula Eq. (45) is turned into a semiclassical one by replacing the term $f\mathbf{v}$ with the summation of contributions from all single-band manifolds, namely,

$$\mathbf{J}^{\text{Ab}}(\mathbf{x}) = -e \sum_n \int d\mathbf{k} f_n \dot{\mathbf{x}}_n, \quad (47)$$

which is straightforwardly analog to Eq. (45). The superscript Ab for the current reminds of appearance of Abelian Berry curvatures in $\dot{\mathbf{x}}_n$.

Since one focuses only on one band at a time, the band index is often omitted as a convention pointed out in the standard textbook [1]. The results Eqs. (46) and (47) are well established in the literature [1,2,18,19] and we shall reproduce them from the more general developments in Sec. III C.

B. Characters of MSCT

1. The general absence of the phase-space locality

For the case of multiple-band manifolds, regardless if these bands are degenerate or not, the single wave-packet SC-EOM for its center of mass is given by Eq. (42), which requires the explicit knowledge of $\bar{\eta}_a$ governed by Eq. (34). The formal solution to Eq. (34) reads $\bar{\eta}_a(t) = \hat{T} \exp \{-i \int_{t_0}^t d\tau \mathcal{H}_a(\mathbf{x}(\tau), \mathbf{k}(\tau))\} \bar{\eta}_a(t_0)$. The time integral $\int_{t_0}^t d\tau$ says that $\bar{\eta}_a(t)$ depends not only on $(\mathbf{x}(t), \mathbf{k}(t))$

but also on the passed trajectories of $(\mathbf{x}(\tau), \mathbf{k}(\tau))$ for τ in the time interval between some initial time t_0 and t . Therefore, the center-of-mass velocity $\dot{\mathbf{x}}$ according to Eq. (42), which evaluates on $\bar{\eta}_a(t)$, in general also depends on these passed trajectories of the center of mass and cannot be a pure function of its present coordinate in the phase space. In other words, the full coherent dynamics of band pseudospin by Eq. (34) renders the loss of the phase-space locality for the center of mass by Eq. (42). This defining feature of nonadiabatic wave-packet dynamics has been demonstrated concretely with a narrow-gap Dirac cone [55].

Note that by the wave-packet transport theory established in the single-band adiabatic regime, the density of states in the phase space has a Berry-curvature-dependent correction which has been derived utilizing the availability of phase-space locality [13]. This correction can play a role in thermal transport and magnetization current within the adiabatic regime [37]. Nevertheless, in the nonadiabatic regime, due to the inevitable loss of phase-space locality, we do not discuss such a correction here.

2. The mass and velocity are not two distinct properties

For an ensemble of wave packets, several wave packets can have the same center of mass while occupying different band states. The most general way of expressing such an occupation configuration with the center of mass at (\mathbf{x}, \mathbf{k}) is via a density operator $\rho(\mathbf{x}, \mathbf{k})$.

We introduce the creation (annihilation) operator a_m^\dagger (a_m) that creates (annihilates) an electron on the bare band m carrying the momentum $\hbar\mathbf{k}$ with the wave-packet center \mathbf{x} . With ρ given, the total occupation number at that phase-space point is $\bar{N} = \sum_m \text{tr}(\rho a_m^\dagger a_m)$. The sum of all wave packets' velocity $\langle \dot{\mathbf{x}} \rangle$ and the force $\hbar\langle \dot{\mathbf{k}} \rangle$ then reads

$$\langle \dot{\mathbf{x}} \rangle = \text{tr}(\rho \hat{V}_M), \quad (48a)$$

and

$$\hbar\langle \dot{\mathbf{k}} \rangle = (-e)\bar{N}\mathbf{E} + \mathbf{F}^R, \quad (48b)$$

with

$$\mathbf{F}^R = \text{tr}(\rho \hat{\mathbf{F}}_M), \quad (48c)$$

in which

$$\hat{V}_M = \sum_{m,l} \langle \bar{u}_m | \frac{\partial \mathcal{H}^c}{\partial \hbar\mathbf{k}} | \bar{u}_l \rangle a_m^\dagger a_l, \quad (49)$$

and

$$\hat{\mathbf{F}}_M = - \sum_{m,l} \langle \bar{u}_m | \frac{\partial \mathcal{H}^c}{\partial \mathbf{x}} | \bar{u}_l \rangle a_m^\dagger a_l \quad (50)$$

are, respectively, the velocity and the force operators extended to the second quantization form. Here the trace operator, $\text{tr}(\cdot)$, is within the band space.

In the language of a PSF, the fluid then has a velocity which has position components given by Eq. (48a) and momentum components by Eq. (48b). The carrier current density then reads

$$\mathbf{J}(\mathbf{x}) = -e \int d\mathbf{k} \langle \dot{\mathbf{x}} \rangle. \quad (51)$$

In SSCT [Eqs. (46) and (47)], the band occupation f_n is analog to the PSF's mass. However, for MSCT with Eq. (51), the carrier distribution with respect to the bands (PSF's mass) has already been taken into account in the definition of $\langle \dot{\mathbf{x}} \rangle$ (PSF's velocity) given by Eqs. (48) through ρ . The clear distinction between the two properties, mass and velocity, of a PSF, thus exists only for SSCT but not for MSCT.

3. Subtlety in extending SSCT to MSCT

A multiple-band manifold with N_a bands can be filled by N wavepackets with $N \leq N_a$. The j th wavepacket has the velocity $\dot{\mathbf{x}}_j$. The sum of N wavepackets' velocity is $\langle \dot{\mathbf{x}} \rangle = \sum_{j=1}^N \dot{\mathbf{x}}_j$. For each wavepacket, one then needs to evolve Eq. (42) to determine $\dot{\mathbf{x}}_j$ which requires the knowledge of the band pseudospin from Eq. (34). This complication is not present for SSCT. Even if the velocity of each wavepacket is obtained, the calculation of the current by Eq. (51) is still hindered by the loss of phase-space locality discussed in Sec. III B 1.

The situation can be much simplified under the following restrictions. We first assume that all the N_a active bands are degenerate over the whole Brillouin zone (BZ) and fully occupied $N = N_a$. Under these conditions, Eq. (51) upon the substitution of $\langle \dot{\mathbf{x}} \rangle = \sum_{j=1}^{N_a} \dot{\mathbf{x}}_j$, where $\dot{\mathbf{x}}_j$ is found by Eq. (42) for the j th wave packet, then reads [61]

$$J_\alpha^{\text{nAb}}(\mathbf{x}) = e \int d\mathbf{k} \sum_{j=1}^{N_a} \sum_{\beta} \left[\langle \mathcal{F}^{k_\alpha x_\beta} \rangle_a \left\langle \frac{\partial \mathcal{H}_a^c}{\partial k_\beta} \right\rangle_a - \langle \mathcal{F}^{k_\alpha x_\beta} \rangle_a \left(\frac{e}{\hbar} E_\beta + \left\langle \frac{\partial \mathcal{H}_a^c}{\partial x_\beta} \right\rangle_a \right) \right]. \quad (52)$$

The superscript nAb has been added to the current for indicating the appearance of non-Abelian Berry curvatures. Equation (52) can be further simplified by removing the spatial textures, namely, $\mathcal{F}^{k_\alpha x_\beta} = 0$ and $\langle \partial \mathcal{H}_a^c / \partial x_\beta \rangle_a = 0$, leading to

$$J_\alpha^{\text{nAb}} = -\frac{e^2}{\hbar} \sum_{\beta} \int d\mathbf{k} \text{Tr}(\mathcal{F}^{k_\alpha k_\beta}) E_\beta, \quad (53)$$

which is a known expression for the Hall current in terms of the trace of the $N_a \times N_a$ non-Abelian Berry curvature matrix [22]. Here \mathbf{J}^{nAb} does not depend on \mathbf{x} since spatial variations have been removed. Equation (53) will be reproduced in Sec. III C.

If a relevant multiple-band manifold is only partially filled (as exemplified in the third column of Fig. 1), where nonadiabatic dynamics matters, then straightforward extension of SSCT to MSCT does not help to evaluate Eq. (51) in general. Nevertheless, the formulation of Eqs. (48) and (51) indicates that as long as one is able to obtain a proper density matrix ρ , the explicit evaluation of the semiclassical current expression using Eq. (51) is still feasible. In fact, finding the density matrix suitable for an electron gas in transport scenarios is the mission targeted by the quantum kinetic theory [62–65]. Instead of being fully quantum with involved microscopic details, the present paper aims to provide a phenomenological shortcut to a steady-state density matrix for semiclassically computing the current.

C. A nonadiabatic semiclassical transport theory

1. The decoherence and the hybridized bands

The steady state described by Eq. (46) as a statistical mixture of populations on a number of bands adiabatically treated in the framework of SSCT has implied the absence of the interband coherence. This has important implication for the steady state in general. In a companion work [55], we have shown that a finite electric field can coherently couple the two branches of a Dirac cone as a nonperturbation effect and the fully coherent band-pseudospin dynamics does not result in a steady-state current. Henceforth, for obtaining the steady-state current in the nonadiabatic regime, the decoherence should be manifested.

Here we briefly recall Ref. [55] for the results of such decoherence. We start from the EOM for interband coherence, Eq. (26), and add a noise term to $\bar{\mathcal{H}}$, the moving-frame effective Hamiltonian given by Eq. (27). By applying the standard Born-Markov decoherence theory for solving the steady-state density matrix for the band state, we find that the steady-state density matrix is diagonal in the eigenbasis of $\bar{\mathcal{H}}$, referred to here as the hybridized bands since they are hybridization of the original bands. The verification of using the hybridized bands as the basis for decoherence will be further discussed later. Here we first have to find these hybridized bands explicitly under the influence of spatial textures.

We denote the hybridized bands by $|u_i\rangle$, namely,

$$\bar{\mathcal{H}}|u_i\rangle = \mathcal{E}_i|u_i\rangle, \quad (54)$$

where i indexes a hybridized band with the corresponding energy \mathcal{E}_i . Equation (54) is for full bands and we will discuss later about focusing on one manifold. With the spatial textures, the off-diagonal hybridization coupling $\bar{\mathcal{H}}_{n,m} = V_{n,m}$ for $n \neq m$ given by Eq. (28) involves the unknown band state because the determination of the center-of-mass $(\dot{\mathbf{x}}, \dot{\mathbf{k}})$ in $V_{n,m}$ relies on it [see Eqs. (19)–(21)]. The eigenstates of $\bar{\mathcal{H}}$ thus depend on the band occupations determined by the decoherence, bringing in additional complications for self-consistently finding the wave functions of the hybridized bands. Indeed, the present description of the spatial textures relies on the local view which is only available when the spatial variation is very smooth. Therefore, we ignore the contributions of spatial variations to interband transitions and approximate $V_{n,m}$ by

$$V_{n,m} \approx -[\bar{\mathcal{R}}\mathbf{k}]_{n,m} \cdot (-e\mathbf{E}), \quad (55)$$

concentrating on the nonadiabatic effect due to the electric field only. Since the local Hamiltonian, \mathcal{H}^c , depends on \mathbf{x} , then the \mathbf{x} dependence is retained in its eigenstate $|\bar{u}_n\rangle$ and $[\bar{\mathcal{R}}\mathbf{k}]_{n,m} = \langle \bar{u}_n | i \partial \bar{u}_m / \partial \mathbf{k} \rangle$, the approximation Eq. (55) still keeps the dependence on \mathbf{x} of $V_{n,m}$.

2. Formulating the current for MSCT

For SSCT, Eq. (46), obtained by the standard kinetic theory [1], is a statistical mixture among the original bands. Analogously in MSCT, with the electric field hybridizing the original bands and the noise eliminating coherence between the hybridized bands, we have a statistical mixture among the

hybridized bands, namely,

$$\text{tr}(\rho c_i^\dagger c_j) = \delta_{i,j} g_i, \quad (56)$$

where c_i^\dagger creates an electron on the hybridized band i . The explicit form of occupation number g_i is found through a route similar to the kinetic theory for SSCT (see Appendix for details) and is given by

$$g_i = g_i^0 + \delta g_i, \quad (57a)$$

with

$$g_i^0 = \frac{1}{e^{(\mathcal{E}_i - \mu)/k_B T} + 1} \quad (57b)$$

and

$$\delta g_i = -\tau \left[\frac{\partial g_i^0}{\partial \mathbf{x}} \cdot \tilde{\mathbf{v}}_i + \frac{\partial g_i^0}{\partial \hbar \mathbf{k}} \cdot (-e\mathbf{E} + \tilde{\mathbf{F}}_i) \right], \quad (57c)$$

in which

$$\tilde{\mathbf{v}}_i = \langle u_i | \frac{\partial \mathcal{H}^c}{\partial \hbar \mathbf{k}} | u_i \rangle \quad (58a)$$

and

$$\tilde{\mathbf{F}}_i = -\langle u_i | \frac{\partial \mathcal{H}^c}{\partial \mathbf{x}} | u_i \rangle. \quad (58b)$$

Substituting Eq. (56) into Eqs. (48) with the aid of Eqs. (58), one obtains

$$\langle \dot{\mathbf{x}} \rangle = \sum_i g_i \tilde{\mathbf{v}}_i, \quad (59)$$

which can be further substituted into Eq. (51) for the final computation of the steady-state current as

$$\mathbf{J}(\mathbf{x}) = -e \sum_i \int d\mathbf{k} g_i \tilde{\mathbf{v}}_i. \quad (60)$$

Given a chemical potential μ and a temperature T , the semi-classical formulas Eqs. (57)–(60) enable the calculation of the currents for multiple bands without the ambiguity discussed in Sec. III B.

Since Eq. (54) behind Eqs. (57)–(60) is for the full-band description, we impose the separation of the full bands into different manifolds introduced in Sec. II B. $\bar{\mathcal{H}}_a$, the projection of $\bar{\mathcal{H}}$ in Eq. (27) on the active manifold, has eigenstates $|u_i^0\rangle$ and eigenenergies \mathcal{E}_i^0 , namely,

$$\bar{\mathcal{H}}_a |u_i^0\rangle = \mathcal{E}_i^0 |u_i^0\rangle. \quad (61)$$

Note that $|u_i^0\rangle$ contains the electric field to all orders. Given the remoteness of the r bands, the hybridized bands as the eigenstates in Eq. (54) are then found by treating a - r couplings, $V_{m,l}$ with $m \in a$ and $l \in r$ in $\bar{\mathcal{H}}$ of Eq. (27), as perturbations to the unperturbed eigenstates of $|u_i^0\rangle$. That means the state vector in Eqs. (58) is given by $|u_i\rangle = |u_i^0\rangle + |\delta u_i\rangle$, where the perturbation correction reads $|\delta u_i\rangle = \sum_{l \in r} \sum_{m \in a} \frac{-V_{l,m} \bar{\eta}_m^{(i)}}{\mathcal{E}_l^0 - \mathcal{E}_i^0} |\bar{u}_l\rangle$, where $\bar{\eta}_m^{(i)} = \langle \bar{u}_m | u_i^0 \rangle$ is found from the diagonalization of Eq. (61) with the approximation Eq. (55). Substituting this $|u_i\rangle$ into Eqs. (58), we obtain

$$\tilde{v}_{i\alpha} = \tilde{v}_{i\alpha}^0 + \frac{e}{\hbar} \sum_{\beta} \langle \mathcal{F}^{k_a k_\beta} \rangle_a^{(i)} E_\beta \quad (62a)$$

and

$$\tilde{F}_{i\alpha} = \tilde{F}_{i\alpha}^0 - e \sum_{\beta} \langle \mathcal{F}^{x_{\alpha}k_{\beta}} \rangle_a^{(i)} E_{\beta}, \quad (62b)$$

where

$$\tilde{v}_{i\alpha}^0 = \langle u_i^0 | \frac{\partial \mathcal{H}_a^c}{\partial \hbar k_{\alpha}} | u_i^0 \rangle, \quad \tilde{F}_{i\alpha}^0 = -\langle u_i^0 | \frac{\partial \mathcal{H}_a^c}{\partial x_{\alpha}} | u_i^0 \rangle \quad (62c)$$

for the α th component of $\tilde{\mathbf{v}}_i$ and $\tilde{\mathbf{F}}_i$, respectively. Here,

$$\langle \mathcal{F}^{\lambda_{\alpha}k_{\beta}} \rangle_a^{(i)} = \sum_{n,m \in a} (\tilde{\eta}_n^{(i)})^* \mathcal{F}_{n,m}^{\lambda_{\alpha}k_{\beta}} \tilde{\eta}_m^{(i)}, \quad (63)$$

with λ_{α} taken to be x_{α} or k_{α} .

We now discuss the relation between the MSCT expressed by Eqs. (57)–(60) and the known result Eq. (53) (obtained without spatial textures, see Sec. III B 3). We leave the discussions for spatial textures and comparison with SSCT to Sec. III C 3. Within a multiple-band manifold, the first term of Eq. (62a) can be decomposed as $\tilde{\mathbf{v}}_i^0 = \tilde{\mathbf{v}}_{b,i}^0 + \tilde{\mathbf{v}}_{h,i}^0$, where $\tilde{\mathbf{v}}_{b,i}^0 = \sum_{n \in a} |\tilde{\eta}_n^{(i)}|^2 \partial \varepsilon_n / \partial (\hbar \mathbf{k})$ and $\tilde{\mathbf{v}}_{h,i}^0 = \sum_{n \in a} \sum_{m \neq n \in a} (\tilde{\eta}_n^{(i)})^* \langle \tilde{u}_n | \partial \mathcal{H}_a^c / \partial (\hbar \mathbf{k}) | \tilde{u}_m \rangle \tilde{\eta}_m^{(i)}$. The result of Eq. (53) in Sec. III B is obtained under the assumptions that the active bands are degenerate over the entire BZ and fully occupied. Under this degenerate condition, $\tilde{\mathbf{v}}_{h,i}^0 = 0$ by Eq. (12) and $\tilde{\mathbf{v}}_i^0 = \tilde{\mathbf{v}}_{b,i}^0$. The full occupancy condition, $g_i = 1$ for all $i \in a$, then gives $\int d\mathbf{k} g_i \tilde{\mathbf{v}}_i^0 = 0$, leaving the second term of Eq. (62a) to be the only nonvanishing contribution to \mathbf{J} and turns Eq. (60) to be Eq. (53).

Note that by Eqs. (58), the second term of Eq. (62a) comes from a perturbation correction, as $\langle u_i^0 | \partial \mathcal{H}_a^c / \partial (\hbar \mathbf{k}) | \delta u_i \rangle + \text{c.c.}$. If other manifolds are very remote from the active one such that the correction is negligible, then this second term of Eq. (62a) can just be ignored. In this case, the energy splitting among the original bands (and henceforth a nonzero anomalous velocity $\tilde{\mathbf{v}}_{h,i}^0 \neq 0$) becomes crucial to current. This is important when the active bands are only degenerate at isolated points but not the entire BZ. In an associated study [55], we considered a model of two bands given by a gapped Dirac cone of small gap size. The coupling to bands beyond the Dirac cone has been completely ignored, keeping only the intramanifold hybridization. We found that the current arising from the anomalous velocity $\tilde{\mathbf{v}}_{h,i}^0$ manifests the underlying nonadiabatic dynamics and conveys a nonperturbative nonlinear valley Hall effect in the absence of the spatial textures. The present establishment Eqs. (57)–(60) also includes the possibility to take into account the spatial textures.

3. The spatial textures

Here we discuss subtle issues related to the presence of spatial textures. We compare the spatial texture effects obtained from Eqs. (57)–(60) with that obtained by Eqs. (46) and (47) summarized in Sec. III A 2 for SSCT.

Note that SSCT is arrived at when the electric field is infinitesimal. The bands are only weakly hybridized and the off-diagonals of Eq. (27) are treated as perturbation in the diagonalization of $\tilde{\mathcal{H}}$. Therefore, the original band index n remains a good quantum number for labeling a weakly hybridized band in Eqs. (57)–(60). To the first order of the electric field, the band energies are $\mathcal{E}_n = \varepsilon_n$, leading to $g_n^0 = f_n^0$

in Eq. (57b). We then write Eq. (57a) as $g_n = f_n^0 + \delta g_n$ to be compared directly with Eq. (46a), $f_n = f_n^0 + \delta f_n$. Explicitly, these nonequilibrium deviations read

$$\delta g_n = -\tau \frac{\partial f_n^0}{\partial \varepsilon_n} \{-\mathbf{F}_{b,n} \cdot \tilde{\mathbf{v}}_n + \mathbf{v}_{b,n} \cdot (-e\mathbf{E} + \tilde{\mathbf{F}}_n)\}, \quad (64)$$

$$\delta f_n = -\tau \frac{\partial f_n^0}{\partial \varepsilon_n} \{-\mathbf{F}_{b,n} \cdot \dot{\mathbf{x}}_n + \mathbf{v}_{b,n} \cdot \hbar \dot{\mathbf{k}}_n\}, \quad (65)$$

where $\mathbf{v}_{b,n} = \partial \varepsilon_n / \partial \hbar \mathbf{k}$ is the normal velocity of the band, and

$$\mathbf{F}_{b,n} = -\frac{\partial \varepsilon_n}{\partial \mathbf{x}} \quad (66)$$

is the force directly associated with the spatial variation of the dispersion. Comparing Eq. (64) with Eq. (65), we see that $\tilde{\mathbf{v}}_n$ and $-e\mathbf{E} + \tilde{\mathbf{F}}_n$ play the roles comparable to $\dot{\mathbf{x}}_n$ and $\hbar \dot{\mathbf{k}}_n$, respectively. We will see that at $\mathbf{E} = 0$, $\delta g_n = 0$ while $\delta f_n \neq 0$ due to terms of second-order derivatives in \mathbf{x} .

In what follows, $\overleftrightarrow{\Omega}_n^{KX}$ denotes a matrix whose elements are defined by $[\overleftrightarrow{\Omega}_n^{KX}]_{\alpha,\beta} = \Omega_n^{k_{\alpha},x_{\beta}}$ [see Eq. (44)] with α, β indexing the spatial directions so $\overleftrightarrow{\Omega}_n^{KX}$ acts on vectors in real space. Similar definitions are applied to $\overleftrightarrow{\Omega}_n^{XX}$, $\overleftrightarrow{\Omega}_n^{KK}$, and $\overleftrightarrow{\Omega}_n^{XK}$. Reducing the number of bands in the active manifold for Eqs. (62) to one, we have

$$\tilde{\mathbf{v}}_n = \mathbf{v}_{b,n} + \mathbf{v}_{h,n} \quad (67a)$$

and

$$\tilde{\mathbf{F}}_n = \mathbf{F}_{b,n} + \mathbf{F}_{h,n}, \quad (67b)$$

where

$$\mathbf{v}_{h,n} = -\frac{e}{\hbar} \overleftrightarrow{\Omega}_n^{KK} \mathbf{E} \quad (67c)$$

is the familiar anomalous velocity due to textures of Bloch bands in momentum space, and

$$\mathbf{F}_{h,n} = -e \overleftrightarrow{\Omega}_n^{XK} \mathbf{E} \quad (67d)$$

is termed the anomalous force with the Berry curvature $\overleftrightarrow{\Omega}_n^{XK}$ involved, discriminating itself from the "normal" force $\mathbf{F}_{b,n}$, Eq. (66). Note that when $\mathbf{E} = 0$, Eqs. (67) reduce to $\tilde{\mathbf{v}}_n = \mathbf{v}_{b,n}$ and $\tilde{\mathbf{F}}_n = \mathbf{F}_{b,n}$. Consequently, $\delta g_n = 0$ in Eq. (64) and with $\int d\mathbf{k} f_n^0 \mathbf{v}_{b,n} = 0$, Eq. (60) gives $\mathbf{J} = 0$ at $\mathbf{E} = 0$. Equations (57)–(60) thus ensure zero current when no external field is applied.

Next we turn to Eq. (65), which is extracted from Eq. (46), and consider $\dot{\mathbf{x}}_n$ and $\hbar \dot{\mathbf{k}}_n$ up to the same order of the small parameter ϵ [cf. Eq. (37)]. The solution to Eqs. (43) for $(\dot{\mathbf{x}}_n, \hbar \dot{\mathbf{k}}_n)$ reads

$$\dot{\mathbf{x}}_n = \tilde{\mathbf{v}}_n + \delta \tilde{\mathbf{v}}_n \quad (68a)$$

and

$$\hbar \dot{\mathbf{k}}_n = -e\mathbf{E} + \tilde{\mathbf{F}}_n + \delta \tilde{\mathbf{F}}_n, \quad (68b)$$

where

$$\delta \tilde{\mathbf{v}}_n = -\overleftrightarrow{\Omega}_n^{KX} \mathbf{v}_{b,n} - \overleftrightarrow{\Omega}_n^{KK} \mathbf{F}_{b,n} / \hbar \quad (68c)$$

and

$$\delta \tilde{\mathbf{F}}_n = \hbar \overleftrightarrow{\Omega}_n^{XX} \mathbf{v}_{b,n} + \overleftrightarrow{\Omega}_n^{XK} \mathbf{F}_{b,n}. \quad (68d)$$

Substituting Eqs. (68) into Eq. (65), one obtains

$$\delta f_n = \delta g_n + \delta f'_n, \quad (69a)$$

where

$$\delta f'_n = -\tau \frac{\partial f_n^0}{\partial \varepsilon_n} (-\mathbf{F}_{b,n} \cdot \delta \tilde{\mathbf{v}}_n + \mathbf{v}_{b,n} \cdot \delta \tilde{\mathbf{F}}_n). \quad (69b)$$

Without spatial textures, namely, $\overleftrightarrow{\Omega}_n^{KX} = \overleftrightarrow{\Omega}_n^{XX} = 0$ and $\mathbf{F}_{b,n} = 0$, then Eqs. (68) and (69) give $\delta \tilde{\mathbf{v}}_n = 0$ and $\delta \tilde{\mathbf{F}}_n = 0$ with $\dot{\mathbf{x}}_n = \tilde{\mathbf{v}}_n$, $\hbar \dot{\mathbf{k}}_n = -e\mathbf{E} + \tilde{\mathbf{F}}_n$ so $\delta f'_n = 0$, leading to $\delta f_n = \delta g_n$. Consequently, Eqs. (57) and (60) reduce to Eqs. (46) and (47).

With spatial textures under the smooth spatial variation approximation Eq. (55), $\tilde{\mathbf{v}}_i$ is zeroth order and $\tilde{\mathbf{F}}_i$ is first order in the derivative of \mathbf{x} , respectively, by Eqs. (58). Therefore, continuing the discussion for single-band manifolds, δg_n in Eq. (64) is first order in $\partial/\partial \mathbf{x}$. Comparing Eq. (69) with Eq. (64), we find $\delta f_n = \delta g_n$ by discarding $\delta f'_n$ which is second order in the derivative of \mathbf{x} . This corresponds to neglecting $\delta \tilde{\mathbf{v}}_n$ and $\delta \tilde{\mathbf{F}}_n$ in Eqs. (68a) and (68b), recovering $\dot{\mathbf{x}}_n = \tilde{\mathbf{v}}_n$ and $\hbar \dot{\mathbf{k}}_n = -e\mathbf{E} + \tilde{\mathbf{F}}_n$. We thus conclude that at $\mathbf{E} = 0$, Eq. (64) gives $\delta g_n = 0$ and therefore also zero current [see the discussions below Eqs. (67)]. Meanwhile, with $\mathbf{E} = 0$, the conventional SSCT described by Eq. (65) [rewritten as Eq. (69)] gives $\delta f_n = \delta f'_n \neq 0$, anticipating a nonzero current due to a nonvanishing deviation from equilibrium $\delta f'_n$ caused by spatial inhomogeneity, second order in the derivative of \mathbf{x} .

When $\mathbf{E} \neq 0$, the effect of spatial textures will be manifested. Plugging Eqs. (67) in Eq. (64) gives

$$\delta g_n = \delta g_n^b + \delta g_n^h, \quad (70a)$$

where

$$\delta g_n^b = -\tau \frac{\partial f_n^0}{\partial \varepsilon_n} \mathbf{v}_{b,n} \cdot (-e\mathbf{E}) \quad (70b)$$

comes from the normal contribution from the normal velocity $\mathbf{v}_{b,n}$ and the electric force $(-e\mathbf{E})$ and

$$\delta g_n^h = -\tau \frac{\partial f_n^0}{\partial \varepsilon_n} \{ \mathbf{v}_{b,n} \cdot \mathbf{F}_{h,n} + \mathbf{F}_{b,n} \cdot \mathbf{v}_{h,n} \}, \quad (70c)$$

is the anomalous contribution involving the anomalous spatial force $\mathbf{F}_{h,n}$ and the familiar anomalous velocity $\mathbf{v}_{h,n}$. Notably, this anomalous contribution δg_n^h is exclusively due to the spatial textures, i.e., requiring $\mathbf{F}_{h,n} \neq 0$, $\mathbf{F}_{b,n} \neq 0$.

Note that the approximation Eq. (55) for smooth spatial variations places no limitation on the magnitude of \mathbf{E} . The finite electric field is responsible for inducing nonadiabatic dynamics for partially filled multiple-band manifolds. As discussed for Eq. (61), $|u_i^0\rangle$ contains all orders of \mathbf{E} . This leads $\tilde{\mathbf{v}}_i$ and $\tilde{\mathbf{F}}_i$ as well as δg_i to also be all orders in \mathbf{E} , reflecting the nonadiabatic dynamics among active bands.

IV. SUMMARY

In Sec. II, concerning the SC-EOM of a single wave packet, we have shown that the same set of EOM, Eqs. (14) and (15), obtained by the Lagrangian variational approach applied to a wave-packet ansatz, can be equally arrived by quantum evolution of the carrier's wave function by the local

Hamiltonian from which the wave packet's center of mass is obtained by quantum expectation values in the form of Eqs. (19) and (20). This SC-EOM for a single wave packet paves the way for discussing nonadiabatic transport for a gas of electrons as an ensemble of wave packets.

In Sec. III, we expounded the difficulty of straightforwardly extending SSCT to MSCT. When there is a multiple-band manifold, the coherent superposition among the several active bands makes the determination of the band state and therefore the velocity expectation value complicated. Due to the loss of phase-space locality of the wave packet's velocity, characteristic to multiple-band manifolds, this also results in the incapacity of semiclassically evaluating the current. We circumvent this obstacle by explicating the loss of interband coherence within the kinetic theory. This leads to the establishment of Eqs. (57)–(60). By inspecting the spatial texture effects, we find that the present MSCT is suitable for smooth spatial variations and ensures that no current can appear unless an external electric field is applied. On the contrary, the known SSCT, Eqs. (46) and (47), has implied a finite current, even in the absence of electric field, that is second order in the spatial derivative.

We now comment on the range of applicability of the MSCT described by Eqs. (57)–(60). First, although we intended the regime where the electric field is finite other than infinitesimal, the magnitude of the electric field should be limited to not push away the electron gas too far from an equilibrium. Otherwise, the kinetic construction with relaxation time approximation simply fails. Second, we have assumed that the scattering rate is independent of the band index. How to go beyond the relaxation time approximation and construct a kinetic theory for the single carrier's dynamics governed by Eqs. (19) and (20) is out of the scope of the present attempt. Albeit these limitations, given the wide uses of the semiclassical transport theory based on Eqs. (46) and (47), the above extension to Eqs. (57)–(60) with finite electric field should also find its place of applications in materials with small gaps as discussed in the Introduction.

ACKNOWLEDGMENTS

The work is supported by the Research Grants Council of Hong Kong (Grants No. HKU17306819 and No. C7036-17W), and the University of Hong Kong (Seed Funding for Strategic Interdisciplinary Research). We thank Hui-Yuan Zheng and Hongyi Yu for useful discussions.

APPENDIX: A KINETIC THEORY FOR MSCT

Here we closely follow the kinetic theory for SSCT [1] and make proper modifications for MSCT to obtain Eq. (57). For SSCT, the evolution of a wave packet according to Eqs. (43) does not lead to interband coherence. The decoherence issue does not appear in the kinetic theory leading to the known SSCT. However, for multiple-band manifolds, a wave packet can evolve to coherent superpositions among bands. Therefore, to construct a proper kinetic theory in this case, one needs to take into account the decoherence explicitly. For the ease of reference, the kinetic theory for SSCT is reviewed in

Appendix A 1. Extension of the kinetic theory from SSCT to MSCT is discussed in Appendix A 2.

1. The building blocks of the kinetic theory

The kinetic theory with the relaxation-time approximation giving rise to Eq. (46) is based on the following assumptions. (i) The scattering within the electron gas maintains it at equilibrium. Given the set of bands indexed by n , a natural choice of the equilibrium distribution function is given by Eq. (46b). (ii) The scattering rate does not depend on the form of the distribution function. (iii) The EOM governing the dynamics of a single carrier free from scattering is given by Eqs. (43) so an electron starting from one band cannot cause nonzero occupations on other bands.

We denote by $f_n(\boldsymbol{\lambda}, t)$ the occupation on a band n at at a phase-space point $\boldsymbol{\lambda} = (\mathbf{x}, \hbar\mathbf{k})$ at time t . The assumption (i) corresponds to decompose f_n as Eq. (46a) in which δf_n is to be derived from assumptions (ii) and (iii). The differential, $df_n(\boldsymbol{\lambda}, t)$, is understood to be the number of electrons gained into the state, $(n, \boldsymbol{\lambda})$. Based on these assumptions, the derivation of Eq. (46c) is divided into the following basic blocks (a)–(d).

(a) Combining assumptions (i) and (ii), one deduces that the number of electrons lost from $(n, \boldsymbol{\lambda})$ from an equilibrium distribution in an infinitesimal time interval dt due to scattering should be compensated by the number of electrons gained into the same state, namely,

$$df_n(\boldsymbol{\lambda}, t) = \frac{dt}{\tau_n(\boldsymbol{\lambda})} f_n^0(\boldsymbol{\lambda}), \quad (\text{A1})$$

in which $\tau_n(\boldsymbol{\lambda})$ is the scattering time whose inverse gives the scattering rate.

(b) The deterministic evolution of Eqs. (43) for a time interval from time t' to t would bring the state $(n, \boldsymbol{\lambda}' = \boldsymbol{\lambda}(t'))$ to the state $(n, \boldsymbol{\lambda} = \boldsymbol{\lambda}(t))$. The electrons occupying the state $(n, \boldsymbol{\lambda})$ at time t are therefore contributed by the no-scattering fraction of those that had occupied $(n, \boldsymbol{\lambda}')$ at time $t' < t$. Denoting by $P_{(n, \boldsymbol{\lambda}')(t, t')}$ as the probability that such evolution can actually be reached without scattering, the occupations at time t are related to all prior times by

$$f_n(\boldsymbol{\lambda}, t) = \int_{t'=-\infty}^{t'=t} df_n(\boldsymbol{\lambda}', t') P_{(n, \boldsymbol{\lambda}')(t, t')}. \quad (\text{A2})$$

(c) The general property of $P_{(n, \boldsymbol{\lambda}')(t, t')}$ is that the no-scattering probability for a time interval from t' to t is smaller than that for a time interval from $t' + dt'$ to t by a factor $(1 - dt'/\tau(\boldsymbol{\lambda}'))$. More explicitly, this reads $P_{(n, \boldsymbol{\lambda}')(t, t')} = P_{(n, \boldsymbol{\lambda}')(t, t' + dt')}(1 - dt'/\tau_n(\boldsymbol{\lambda}'))$ and, consequently,

$$\frac{\partial}{\partial t'} P_{(n, \boldsymbol{\lambda}')(t, t')} = \frac{P_{(n, \boldsymbol{\lambda}')(t, t')}}{\tau_n(\boldsymbol{\lambda}')}. \quad (\text{A3})$$

Furthermore, this no-scattering probability also satisfies

$$P_{(n, \boldsymbol{\lambda}')(t, t)} = 1, \quad (\text{A4a})$$

simply for that when $t = t'$ there is no time for scattering to occur between t' and t and

$$P_{(n, \boldsymbol{\lambda}')(t, -\infty)} = 0 \quad (\text{A4b})$$

for scattering definitely occurs in a long-enough time interval.

(d) Combining Eqs. (A1) and (A3) into Eq. (A2) and performing the resulting integral over dt' via the integration by parts with the boundary condition Eq. (A4), we obtain an intermediate expression

$$f_n(\boldsymbol{\lambda}, t) = f_n^0(\boldsymbol{\lambda}) - \int_{t'=-\infty}^{t'=t} dt' e^{-(t-t')/\tau_n(\boldsymbol{\lambda}')} \left[\frac{d}{dt'} f_n^0(\boldsymbol{\lambda}(t')) \right]. \quad (\text{A5})$$

Assuming further that τ_n is very short so the factor $e^{-(t-t')/\tau_n(\boldsymbol{\lambda}')}$ only contributes significantly when t' is near t , the integrand in Eq. (A5) is then approximated by $\tau_n(\boldsymbol{\lambda}(t')) \approx \tau_n(\boldsymbol{\lambda})$ and $[\frac{d}{dt'} f_n^0(\boldsymbol{\lambda}(t'))] \approx [\frac{d}{dt} f_n^0(\boldsymbol{\lambda}(t))]$, and Eq. (A5) reduces to $f_n(\boldsymbol{\lambda}) = f_n^0(\boldsymbol{\lambda}) - \tau [\frac{d}{dt} f_n^0(\boldsymbol{\lambda}(t))]$, writing simply $\tau = \tau_n(\boldsymbol{\lambda})$, a precursor of Eq. (46). By further expressing $[\frac{d}{dt} f_n^0(\boldsymbol{\lambda}(t))] = \partial f_n^0 / \partial \boldsymbol{\lambda} \cdot \dot{\boldsymbol{\lambda}}_n$, Eq. (46) is recovered. Applying $\partial / \partial t$ to both sides of Eq. (A5) with the short scattering-time approximation, one consistently obtains the stationarity of $f_n(\boldsymbol{\lambda}, t)$, namely, $\partial f_n(\boldsymbol{\lambda}, t) / \partial t = 0$ so $f_n(\boldsymbol{\lambda}, t) = f_n(\boldsymbol{\lambda})$. We are thus led to the SSCT summarized in Sec. III A 2.

2. Constructing the kinetic theory in the nonadiabatic regime

For multiple-band manifolds, given a density matrix $\rho(t)$ at time t , the probability of having a wave packet with band state $|\chi\rangle$ and the center of mass, $\boldsymbol{\lambda} = (\mathbf{x}, \hbar\mathbf{k})$, is given by $g_\chi(\boldsymbol{\lambda}, t) = \text{tr}(\rho(t) a_\chi^\dagger(\boldsymbol{\lambda}) a_\chi(\boldsymbol{\lambda}))$, where $a_\chi^\dagger(\boldsymbol{\lambda})$ creates an electron wave packet of such a state.

Similar to the construction for SSCT in Appendix A 1, here we build a kinetic theory in the nonadiabatic regime from the same assumptions (i) and (ii) as before, with the original bands replaced by the hybridized bands [eigenstates described in Eq. (54)]. Assumption (i) amounts to having Eq. (56) with g_i decomposed as Eq. (57a), but leaving the deviation δg_i unspecified, whose explicit form will be derived here. More crucially, the underlying scattering-free single carrier's SC-EOM are now given by Eqs. (19) and (20), instead of Eqs. (43). This allows nonperturbative interband transitions that create interband coherence.

The loss of coherence among the hybridized bands is accounted as the following. Using $|u_i\rangle$'s as a complete basis set, we have $a_\chi^\dagger = \sum_i \langle u_i | \chi \rangle c_i^\dagger$ and henceforth, $g_\chi = \text{tr}(\rho a_\chi^\dagger a_\chi) = \sum_{i,j} \langle u_i | \chi \rangle \text{tr}(\rho c_i^\dagger c_j) \langle \chi | u_j \rangle$. Combining this with Eq. (56), which expresses no coherence among hybridized bands, we are led to

$$g_\chi(\boldsymbol{\lambda}, t) = \sum_i |\langle u_i | \chi \rangle|^2 g_i(\boldsymbol{\lambda}, t). \quad (\text{A6})$$

We will see that the kinetic theory for MSCT introduced here is in one-to-one correspondence to that of SSCT. The building blocks (a)–(d) in Appendix A 1 become (a')–(d') below, with the additional use of the decoherence consequence, Eq. (A6).

(a') The equilibrium being unaltered by scattering can still be formulated similar to Eq. (A1) by

$$dg_i(\boldsymbol{\lambda}, t) = \frac{dt}{\tau(\boldsymbol{\lambda})} g_i^0(\boldsymbol{\lambda}), \quad (\text{A7})$$

where, for simplicity, we ignored the band dependence of the scattering rate.

(b') The scattering-free evolution guided by Eqs. (19) and (20) generally evolves an electron from a state specified by $(\chi' = \chi(t'), \lambda' = \lambda(t'))$ to a state $(\chi = \chi(t), \lambda = \lambda(t))$. The occupation of a state (χ, λ) at time t is related to all prior times by

$$g_{\chi}(\lambda, t) = \int_{t'=-\infty}^{t'=t} dg_{\chi'}(\lambda', t') P_{(\chi', \lambda')}(t, t'), \quad (\text{A8})$$

where $P_{(\chi', \lambda')}(t, t')$ stands for the probability that a carrier occupying the state (χ', λ') at time t' would not be scattered in the interval between t' and t .

(c') The property that the scattering occurs with a probability proportional to the length of time interval considered is very general. Therefore, by the similarity to Eq. (A3), we have

$$\frac{\partial}{\partial t'} P_{(\chi', \lambda')}(t, t') = \frac{P_{(\chi', \lambda')}(t, t')}{\tau(\lambda')}, \quad (\text{A9})$$

and surely also

$$P_{(\chi', \lambda')}(t, t) = 1 \quad (\text{A10a})$$

and

$$P_{(\chi', \lambda')}(t, -\infty) = 0. \quad (\text{A10b})$$

(d') Similar to the steps prescribed in (d), substituting Eqs. (A7) and (A9) with the boundary conditions Eq. (A10) into Eq. (A8), the integration by parts performed to the integral over dt' leads to an integral equation similar to Eq. (A5). Now on the left-hand side of Eq. (A8), we let $|\chi\rangle = |u_i\rangle$ so $g_{\chi} = g_i$. On the right-hand side of Eq. (A8), we replace $g_{\chi'}$ in the integrand by Eq. (A6). These lead to

$$i(\lambda, t) = g_i^0(\lambda) - \sum_{i'} \int_{t'=-\infty}^{t'=t} dt' e^{-(t-t')/\tau(\lambda')} |\langle u_{i'} | \chi' \rangle|^2 \left[\frac{d}{dt'} g_{i'}^0(\lambda(t')) \right]. \quad (\text{A11})$$

Applying the short scattering-time approximation similar to that discussed after Eq. (A5) with the aid of $\langle u_{i'} | u_i \rangle = \delta_{i', i}$, we are led to Eq. (57) in the main text.

-
- [1] N. W. Ashcroft and N. D. Mermin, *Solid State Physics* (Sounders College, Philadelphia, 1976).
- [2] D. Xiao, M.-C. Chang, and Q. Niu, Berry phase effects on electronic properties, *Rev. Mod. Phys.* **82**, 1959 (2010).
- [3] R. Karplus and J. M. Luttinger, Hall effect in ferromagnetics, *Phys. Rev.* **95**, 1154 (1954);
- [4] J. M. Luttinger, Theory of the Hall effect in ferromagnetic substances, *Phys. Rev.* **112**, 739 (1958).
- [5] E. Adams and E. Blount, Energy bands in the presence of an external force field-II: Anomalous velocities, *J. Phys. Chem. Solids* **10**, 286 (1959).
- [6] T. Jungwirth, Q. Niu, and A. H. MacDonald, Anomalous Hall Effect in Ferromagnetic Semiconductors, *Phys. Rev. Lett.* **88**, 207208 (2002).
- [7] N. Nagaosa, J. Sinova, S. Onoda, A. H. MacDonald, and N. P. Ong, Anomalous Hall effect, *Rev. Mod. Phys.* **82**, 1539 (2010).
- [8] S. Murakami, N. Nagaosa, and S.-C. Zhang, Dissipationless quantum spin current at room temperature, *Science* **301**, 1348 (2003).
- [9] J. Sinova, D. Culcer, Q. Niu, N. A. Sinitsyn, T. Jungwirth, and A. H. MacDonald, Universal Intrinsic Spin Hall Effect, *Phys. Rev. Lett.* **92**, 126603 (2004).
- [10] D. Xiao, W. Yao, and Q. Niu, Valley-Contrasting Physics in Graphene: Magnetic Moment and Topological Transport, *Phys. Rev. Lett.* **99**, 236809 (2007).
- [11] D. Xiao, G.-B. Liu, W. Feng, X. Xu, and W. Yao, Coupled Spin and Valley Physics in Monolayers of MoS₂ and Other Group-VI Dichalcogenides, *Phys. Rev. Lett.* **108**, 196802 (2012).
- [12] D. T. Son and B. Z. Spivak, Chiral anomaly and classical negative magnetoresistance of Weyl metals, *Phys. Rev. B* **88**, 104412 (2013).
- [13] D. Xiao, J. Shi, and Q. Niu, Berry Phase Correction to Electron Density of States in Solids, *Phys. Rev. Lett.* **95**, 137204 (2005).
- [14] M.-C. Chang and Q. Niu, Berry curvature, orbital moment, and effective quantum theory of electrons in electromagnetic fields, *J. Phys.: Condens. Matter* **20**, 193202 (2008).
- [15] E. V. Gorbar, V. A. Miransky, I. A. Shovkovy, and P. O. Sukhachov, Non-Abelian properties of electron wave packets in the Dirac semimetals A₃Bi (A = Na, K, Rb), *Phys. Rev. B* **98**, 045203 (2018).
- [16] J. C. Olson and P. Ao, Nonequilibrium approach to Bloch-Peierls-Berry dynamics, *Phys. Rev. B* **75**, 035114 (2007).
- [17] K. Misaki, S. Miyashita, and N. Nagaosa, Diffusive real-time dynamics of a particle with Berry curvature, *Phys. Rev. B* **97**, 075122 (2018).
- [18] M. C. Chang and Q. Niu, Berry Phase, Hyperorbits, and the Hofstadter Spectrum, *Phys. Rev. Lett.* **75**, 1348 (1995).
- [19] M. C. Chang and Q. Niu, Berry phase, hyperorbits, and the Hofstadter spectrum: Semiclassical dynamics in magnetic Bloch bands, *Phys. Rev. B* **53**, 7010 (1996).
- [20] G. Sundaram and Q. Niu, Wave-packet dynamics in slowly perturbed crystals: Gradient corrections and Berry-phase effects, *Phys. Rev. B* **59**, 14915 (1999).
- [21] D. Culcer, Y. Yao, and Q. Niu, Coherent wave-packet evolution in coupled bands, *Phys. Rev. B* **72**, 085110 (2005).
- [22] R. Shindou and K. I. Imura, Noncommutative geometry and non-Abelian Berry phase in the wave-packet dynamics of Bloch electrons, *Nucl. Phys. B* **720**, 399 (2005).
- [23] B. Hunt, J. D. Sanchez-Yamagishi, A. F. Young, M. Yankowitz, B. J. LeRoy, K. Watanabe, T. Taniguchi, P. Moon, M. Koshino, P. Jarillo-Herrero, and R. C. Ashoori, Massive Dirac fermions and Hofstadter butterfly in a van der Waals heterostructure, *Science* **340**, 1427 (2013).
- [24] C. R. Woods, L. Britnell, A. Eckmann, R. S. Ma, J. C. Lu, H. M. Guo, X. Lin, G. L. Yu, Y. Cao, R. V. Gorbachev, A. V. Kretinin, J. Park, L. A. Ponomarenko, M. I. Katsnelson, Yu. N. Gornostyrev, K. Watanabe, T. Taniguchi, C. Casiraghi, H.-J. Gao, A. K. Geim, and K. S. Novoselov, Commensurate-incommensurate transition in graphene on hexagonal boron nitride, *Nat. Phys.* **10**, 451 (2014).
- [25] D. Zhang, M. Shi, T. Zhu, D. Xing, H. Zhang, and J. Wang, Topological axion States in the Magnetic Insulator MnBi₂Te₄

- with the Quantized Magnetoelectric Effect, *Phys. Rev. Lett.* **122**, 206401 (2019).
- [26] J. Li, C. Wang, Z. Zhang, B.-L. Gu, W. Duan, and Y. Xu, Magnetically controllable topological quantum phase transitions in the antiferromagnetic topological insulator MnBi_2Te_4 , *Phys. Rev. B* **100**, 121103(R) (2019).
- [27] J. Li, Y. Li, S. Du, Z. Wang, B.-L. Gu, S.-C. Zhang, K. He, W. Duan, and Y. Xu, Intrinsic magnetic topological insulators in van der Waals layered MnBi_2Te_4 -family materials, *Sci. Adv.* **5**, eaaw5685 (2019).
- [28] C. Liu, Y. Wang, H. Li, Y. Wu, Y. Li, J. Li, K. He, Y. Xu, J. Zhang, and Y. Wang, Robust axion insulator and Chern insulator phases in a two-dimensional antiferromagnetic topological insulator, *Nat. Mater.* **19**, 522 (2020).
- [29] S. A. Yang, G. S. D. Beach, C. Knutson, D. Xiao, Q. Niu, M. Tsoi, and J. L. Erskine, Universal Electromotive Force Induced by Domain Wall Motion, *Phys. Rev. Lett.* **102**, 067201 (2009).
- [30] K. Everschor-Sitte and M. Sitte, Real-space Berry phases: Skyrmion soccer (invited), *J. Appl. Phys.* **115**, 172602 (2014).
- [31] C. Zhang, C.-P. Chuu, X. Ren, M.-Y. Li, L.-J. Li, C. Jin, M.-Y. Chou, and C.-K. Shih, Interlayer couplings, moiré patterns, and 2D electronic superlattices in $\text{MoS}_2/\text{WSe}_2$ hetero-bilayers, *Sci. Adv.* **3**, e1601459 (2017).
- [32] Y. Pan, S. Fölsch, Y. Nie, D. Waters, Y.-C. Lin, B. Jariwala, K. Zhang, K. Cho, J. A. Robinson, and R. M. Feenstra, Quantum-confined electronic states arising from the moiré pattern of $\text{MoS}_2\text{-WSe}_2$ heterobilayers, *Nano Lett.* **18**, 1849 (2018).
- [33] R. Bistritzer and A. H. MacDonald, moiré bands in twisted double-layer graphene, *Proc. Natl. Acad. Sci. USA* **108**, 12233 (2011).
- [34] M. Kindermann, B. Uchoa, and D. Miller, Zero-energy modes and gate-tunable gap in graphene on hexagonal boron nitride, *Phys. Rev. B* **86**, 115415 (2012).
- [35] J. Wallbank, M. Mucha-Kruczynski, X. Chen, and V. Fal'ko, moiré superlattice effects in graphene/boron-nitride van der Waals heterostructures, *Ann. Phys.* **527**, 359 (2015).
- [36] N. R. Cooper, B. I. Halperin, and I. M. Ruzin, Thermoelectric response of an interacting two-dimensional electron gas in a quantizing magnetic field, *Phys. Rev. B* **55**, 2344 (1997).
- [37] C. Xiao and Q. Niu, Unified bulk semiclassical theory for intrinsic thermal transport and magnetization currents, *Phys. Rev. B* **101**, 235430 (2020).
- [38] J. C. Slater, Electrons in perturbed periodic lattices, *Phys. Rev.* **76**, 1592 (1949).
- [39] J. M. Luttinger, The effect of a magnetic field on electrons in a periodic potential, *Phys. Rev.* **84**, 814 (1951).
- [40] E. I. Blount, in *Solid State Physics*, edited by F. Seitz and D. Turnbull, No. **13** (Academic Press, New York, 1962), p. 305.
- [41] G. H. Wannier, Dynamics of band electrons in electric and magnetic fields, *Rev. Mod. Phys.* **34**, 645 (1962).
- [42] J. Zak, Dynamics of electrons in solids in external fields, *Phys. Rev.* **168**, 686 (1968).
- [43] R. Shindou and L. Balents, Gradient expansion approach to multiple-band Fermi liquids, *Phys. Rev. B* **77**, 035110 (2008).
- [44] M. F. Lapa and T. L. Hughes, Semiclassical wave packet dynamics in nonuniform electric fields, *Phys. Rev. B* **99**, 121111 (2019).
- [45] T. Stedman, C. Timm, and L. M. Woods, Multiband effects in equations of motion of observables beyond the semiclassical approach, *New J. Phys.* **21**, 103007 (2019).
- [46] G. Panati, H. Spohn, and S. Teufel, Effective dynamics for Bloch electrons: Peierls substitution and beyond, *Commun. Math. Phys.* **242**, 547 (2003).
- [47] P. Gosselin, F. Ménas, A. Bérard, and H. Mohrbach, Semiclassical dynamics of electrons in magnetic Bloch bands: A Hamiltonian approach, *Europhys. Lett.* **76**, 651 (2006).
- [48] K. Y. Bliokh, Topological spin transport of a relativistic electron, *Europhys. Lett.* **72**, 7 (2005).
- [49] Ö. F. Dayi, Spin dynamics with non-Abelian Berry gauge fields as a semiclassical constrained Hamiltonian system, *J. Phys. A: Math. Theor.* **41**, 315204 (2008).
- [50] E. Bettelheim, Derivation of one-particle semiclassical kinetic theory in the presence of non-Abelian Berry curvature, *J. Phys. A* **50**, 415303 (2017).
- [51] One can let the vector potential be dependent on \mathbf{x}_c , namely, $\mathbf{A} = \mathbf{A}(t, \mathbf{x}_c)$. Then the equation for \mathbf{k}_c will be changed from Eq. (20) to $\hbar\dot{\mathbf{k}}_c = (-e)(\mathbf{E} + \dot{\mathbf{x}}_c \times \mathbf{B}) - \langle \chi | \partial \mathcal{H}^c / \partial \mathbf{x}_c | \chi \rangle$, where $\mathbf{B} = \nabla \times \mathbf{A}$, while other equations remain the same.
- [52] D. J. Thouless, M. Kohmoto, M. P. Nightingale, and M. den Nijs, Quantized Hall Conductance in a Two-Dimensional Periodic Potential, *Phys. Rev. Lett.* **49**, 405 (1982).
- [53] A. Böhm, H. Koizumi, Q. Niu, J. Zwanziger, and A. Mostafazadeh, *The Geometric Phase in Quantum Systems* (Springer, Berlin, 2003).
- [54] By a different gauge choice of the instantaneous basis $|u_n(\boldsymbol{\lambda})\rangle \rightarrow |u'_n(\boldsymbol{\lambda})\rangle = e^{i\theta_n(\boldsymbol{\lambda})}|u_n(\boldsymbol{\lambda})\rangle$, the coherence phase $\beta_{n,m} \equiv \arg(\eta_n^* \eta_m / |\eta_n^* \eta_m|)$ is also changed, $\beta_{n,m} \rightarrow \beta'_{n,m} = \beta_{n,m} + \theta_n - \theta_m$, where $\boldsymbol{\lambda}$ denotes the center-of-mass ($\mathbf{x}, \hbar\mathbf{k}$). However, with Eqs. (24), the gauge change $|\bar{u}_n(\boldsymbol{\lambda})\rangle \rightarrow |\bar{u}'_n(\boldsymbol{\lambda})\rangle = e^{i\theta_n(\boldsymbol{\lambda})}|\bar{u}_n(\boldsymbol{\lambda})\rangle$ does not alter the value of $\beta_{n,m} \equiv \arg(\bar{\eta}_n^* \bar{\eta}_m / |\bar{\eta}_n^* \bar{\eta}_m|)$.
- [55] M. W.-Y. Tu, C. Li, H. Yu, and W. Yao, Non-adiabatic Hall effect at Berry curvature hot spot, *2D Mater.* **7**, 045004 (2020).
- [56] F. Wilczek and A. Zee, Appearance of Gauge Structure in Simple Dynamical Systems, *Phys. Rev. Lett.* **52**, 2111 (1984).
- [57] N. A. Sinitsyn, Q. Niu, J. Sinova, and K. Nomura, Disorder effects in the anomalous Hall effect induced by Berry curvature, *Phys. Rev. B* **72**, 045346 (2005).
- [58] E. Deyo, L. E. Golub, E. L. Ivchenko, and B. Spivak, Semiclassical theory of the photogalvanic effect in non-centrosymmetric systems, [arXiv:0904.1917v1](https://arxiv.org/abs/0904.1917v1).
- [59] J. E. Moore and J. Orenstein, Confinement-Induced Berry Phase and Helicity-Dependent Photocurrents, *Phys. Rev. Lett.* **105**, 026805 (2010).
- [60] I. Sodemann and L. Fu, Quantum Nonlinear Hall Effect Induced by Berry Curvature Dipole in Time-Reversal Invariant Materials, *Phys. Rev. Lett.* **115**, 216806 (2015).
- [61] Since the degenerate active bands are fully occupied over the whole BZ, the part of the velocity obtained by summing the first term of Eq. (42a) (intramanifold) over all wave packets does not contribute to the current. Only the second term of Eq. (42a), describing the effects from other manifolds, contributes to the current. $\langle \dot{\mathbf{x}} \rangle$ is now obtained by sum-

- ming the second term of Eq. (42a) over all the N_a wave packets. Substituting such $\langle \dot{\mathbf{x}} \rangle$ into Eq. (51) gives $J_\alpha(\mathbf{x}) = e \int d\mathbf{k} \sum_{j=1}^{N_a} \sum_{\beta} [\langle \mathcal{F}^{k_\alpha x_\beta} \rangle_\alpha \dot{x}_\beta + \langle \mathcal{F}^{k_\alpha k_\beta} \rangle_\alpha \dot{k}_\beta]_j$, where J_α is the α th spatial component of \mathbf{J} . To arrive at Eq. (52), $(\dot{\mathbf{x}}, \dot{\mathbf{k}})$ above is found by solving Eq. (42) to the zeroth order of ϵ , Eq. (37), to keep \mathbf{J} to the first order of ϵ .
- [62] W. Kohn and J. M. Luttinger, Quantum theory of electrical transport phenomena, *Phys. Rev.* **108**, 590 (1957).
- [63] F. T. Vasko and O. E. Raichev, *Quantum Kinetic Theory and Applications* (Springer, New York, 2005).
- [64] D. Culcer, A. Sekine, and A. H. MacDonald, Interband coherence response to electric fields in crystals: Berry-phase contributions and disorder effects, *Phys. Rev. B* **96**, 035106 (2017).
- [65] C. Xiao, Z. Z. Du, and Q. Niu, Theory of nonlinear Hall effects: Modified semiclassics from quantum kinetics, *Phys. Rev. B* **100**, 165422 (2019).